Habitable Planet, 2026, 2(2), 303–324

Habitable Planet

Journal Homepage: https://www.sciltp.com/journals/hp

Article

Lateral Variations in Evolution of a Fold-thrust Belt Hinterland: Passive versus Active Behavior of Dominant Internal Thrust Sheets

Gautam Mitra[1], Steven E. Boyer[2], Sanghoon Kwon[3,*], Malay Mukul[4], Zeshan Ismat[5], and Aviva Sussman[6]

[1]Department of Earth and Environmental Sciences, University of Rochester, Rochester, NY 14627, USA
[2]2831 Arrowroot Loop SE, Olympia, WA 98513, USA
[3]Department of Earth System Sciences, Yonsei University, Seoul 03722, Republic of Korea
[4]Department of Earth Sciences, IIT Bombay, Mumbai 400076, India
[5]Department of Earth and Environmental Science, Franklin and Marshall College, Lancaster, PA 17603, USA
[6]Earth and Environmental Sciences, Los Alamos National Laboratory, Los Alamos, NM 87545, USA
[*] Correspondence: skwon@yonsei.ac.kr

ABSTRACT

Critical wedge theory (CWT) explains the large-scale architecture, kinematic evolution and strain distribution of fold-thrust belts (FTBs) for both plastic and Coulomb wedges. During progressive deformation in an FTB wedge, the taper tends to decrease due to a variety of causes. CWT requires continued deformation in the back of the wedge to maintain critical taper in the wedge as a whole. Since the overall taper of the FTB wedge is typically determined by the geometry of a dominant thrust sheet in the hinterland of the FTB, it is the deformation behavior of such a sheet that defines wedge behavior as a whole. After initial emplacement of a dominant hinterland sheet, deformation in the back of the wedge may result in passive uplift and/or translation of the dominant sheet, or it may result in active deformation of the entire back of the wedge. The Sevier fold–thrust belt (FTB) provides an excellent natural example for evaluating these CWT-predicted behaviors based on three decades of structural studies. In summary, the Lewis segment (initial taper $\sim 9^{\circ}$), the Central Utah segment (initial taper $\sim 6^{\circ}$) and the Provo segment (initial taper $\sim 3^{\circ}$) of the Sevier FTB have different initial sedimentary prism geometries and lithotectonic configurations, providing contrasting examples that are end-case scenarios of dominant hinterland sheet behavior both during initial emplacement and during late stage deformation of the back of the wedge as an FTB evolves. Strain data from these three areas are compatible with the interpretive models.

ARTICLE INFO

History:

Received: 24 December 2025
Revised: 01 April 2026
Accepted: 06 May 2026
Published: 12 May 2026

Keywords:

fold-thrust belts;
strain behavior;
passive margin sediments;
structural evolution

Citation:

Mitra, G.; Boyer, S.E.; Kwon, S.; et al. Lateral Variations in Evolution of a Fold-thrust Belt Hinterland: Passive versus Active Behavior of Dominant Internal Thrust Sheets. *Habitable Planet* **2026**, *2*(2), 303–324. https://doi.org/10.63335/j.hp.2026.0040

Research Highlights

- Internal hinterland thrust sheets are dominant structural elements for explaining large-scale FTB evolution.
- Large-scale FTB evolution has lateral variations in terms of passive vs. active behavior of dominant internal thrust sheets.
- The mechanical behavior of internal thrust sheets is governed by multiple factors affecting the orogenic wedge.

1. Introduction

Hinterland thrust sheets play a prominent role in the evolution of most retroarc fold-thrust belts (FTBs) that typically evolve from passive margin sedimentary sequences. The hinterland sheets originate from the thick miogeoclinal portion of the sequence outboard of the shelf–miogeocline hinge and are emplaced along crustal scale ramps onto the shelf [1]. In terms of their sheer size and displacement the hinterland sheets dwarf the rest of the fold-thrust belt [2]. In addition, during the prolonged history of deformation, uplift and erosion, the rocks in these sheets are carried up from intermediate crustal levels in areas with high geothermal gradient up to shallow crustal levels in areas with significantly lower (cratonic) geothermal gradients [3]. This, together with repeated reactivation during successive episodes of thrusting, results in hinterland thrust sheets commonly displaying complex thermal and kinematic histories. The complex structures in these sheets have to be carefully evaluated [4, 5] to understand mechanisms in the hinterland that drive thrusting on to the foreland. Although the details of structural geometry and kinematic evolution of hinterland sheets may vary from one FTB to another, in all cases their continued activity throughout FTB evolution provides the structural elevations and surface slopes necessary to propagate thrusting toward the foreland in an FTB [6].

The structural evolution of an individual hinterland thrust sheet can be affected by a variety of factors that include the following: the geometry of the original sedimentary prism and its lithotectonic configuration, the material properties of the rocks in the sedimentary prism, the geothermal gradient and how it varies from the hinterland to the foreland, the presence or absence of fluids within the tectonic wedge, and the rate of shortening within the fold-thrust belt as a whole. These factors are expected to vary from one orogen to another, but they can also change along strike within a single FTB so that the hinterland evolves differently in different segments along the length of the FTB. The Sevier FTB of the North American Cordillera shows along-strike changes in many of these factors resulting in significant lateral variations in the structural evolution of the FTB.

We have carried out considerable structural mapping, and undertaken detailed outcrop-scale analysis, and microstructural and strain studies in different internal (hinterland) thrust sheets of the Sevier FTB over the past three decades. Here we summarize the data from a number of these studies in the context of the large-scale tectonic setting and discuss their implications for the evolution of hinterland sheets in different segments of the Sevier FTB. The commonalities and contrasts in observed patterns may also serve as useful models for evaluating hinterland thrust sheets in other FTBs.

2. Background

2.1. Wedge Theory

Critical wedge theory [7, 8] provides us with a useful conceptual framework for the large-scale evolution of fold-thrust belts (FTBs). It is now widely accepted that for plastic [7], Coulomb [8] and hybrid, two-layer elastic-frictional (EF)–quasi-plastic (QP) [9] wedges, the taper of the wedge (given by the sum of its surface slope α and its basal dip β) has to reach a critical value for the wedge to slide along its base. A variety of factors can affect the orogenic wedge during its progressive evolution [6]. For example, the shape of the wedge may change due to surface erosion bringing the wedge into the subcritical field. Flexure of the lithosphere due to loading by thrust sheets can also affect wedge taper (by changing both α and β) so that the wedge becomes subcritical. Alternatively, changes in material behavior of the wedge can change the critical taper condition so that the wedge moves off the critical taper line; for example, increase in the strength of the wedge (by strain hardening) or weakening of the base (due to the formation of strain softening mylonites under plastic deformation conditions or as a result of increase in fluid pressure along the base) can depress the critical taper line and cause the wedge to become supercritical.

During the evolution of a backarc FTB, the wedge can respond to short-term supercritical stages by imbrication at the wedge-toe thereby reducing overall taper. Similarly, short-term subcriticality due to erosion can be counteracted by shortening and thickening in internal thrust sheets at the back of the FTB wedge thereby increasing overall taper [6]. More importantly, over the long term, erosion reduces the surface slope component of wedge taper. This requires continued deformation in the back of the wedge throughout the history of evolution of an FTB [10] for the wedge to continue movement along its basal decollement.

Evidence for such continued out-of-sequence reactivation in internal thrust sheets has been described from different parts of the Sevier FTB in the North American

Cordillera [6, 11]. Provenance data from synorogenic sediments [12–14], timing of folding and faulting from structural cross-cutting relationships [3, 4, 6, 15] and uplift histories from fission track data [12, 16] together provide a consistent story for wedge evolution. Geometric analysis and related kinematic restorations also require synchronous thrusting, out-of-sequence imbrication, and thrust reactivation [17–19]; although less reliable for the absolute and relative dating of thrust motions, such geometries may be the only means to extract kinematic evidence in the absence of synorogenic sediments. The evidence suggests that thrusting progresses onto the foreland with time while concomitantly the hinterland continues to be reactivated and uplifted. Major internal (i.e. hinterland) thrust sheets reach large structural elevations and are the dominant contributors of synorogenic sediments to the foreland basin [12].

Internal (hinterland) thrust sheets tend to be significantly larger than external sheets [20], and are lithotectonically stronger than external sheets, being made up of crystalline basement rocks and/or quartz-rich sedimentary rocks [6, 20]. They also tend to show significantly larger translation on their underlying thrust faults and have therefore been referred to as dominant thrust sheets [17]. These large translations are not only geometrically necessary for properly balanced cross-sections [21, 22] but are also required mechanically to drive thrusting on to the foreland during progressive evolution of any FTB [6]. As indicated earlier, these sheets tend to be active over the entire period of evolution of an FTB, so that some parts of the larger translation may accumulate during periods of reactivation after the initial emplacement of the thrust sheet [17].

Thus, the deformation history of internal dominant thrust sheets plays an important role in the evolution of FTBs as a whole [11]. Any backarc FTB may be thought of as being made up of two juxtaposed wedges: a strong, thick rear wedge with larger taper, and a weaker, thinner frontal wedge with lower taper [6]. Shortening and thickening of the rear wedge enhances taper of the wedge as a whole and drives thrusting onto the foreland. Because of the dominant role of the rear wedge in the mechanical evolution of the FTB as a whole it is important to understand the structural evolution of internal thrust sheets at all scales. The actual behavior of the FTB hinterland may vary along strike depending on a variety of factors that influence the deformation of internal thrust sheets.

2.2. Factors Affecting Wedge Evolution

Any retroarc FTB develops from an initial sedimentary prism [1] that most likely formed in a passive margin setting. If we make the simplifying assumption of a basin-filled sedimentary prism (i.e. one with a horizontal top) at the start of deformation, then the underlying basement slope (β) determines the initial taper of the tectonic wedge. Physical and numerical 3-D modeling studies [23–26] show that during initial deformation the back end of the sedimentary prism must shorten and thicken for the wedge to reach critical taper before it starts sliding at its base [7]. Field evidence (e.g. [6]), physical models (e.g. [27, 28]), and numerical models [26, 29] all suggest that this process actually progresses from the back to the front of the wedge through time and thrusting propagates toward the foreland. To simplify calculations, we can visualize the taper enhancing deformation as a one-step process and calculate the minimum shortening required within the wedge for the entire wedge to reach critical taper [11, 30] and related works by the authors. We realize that this approach does not take progressive deformation and surface erosion or other complicating factors into account but it does provide us with first order results that allow us to compare the behavior of tectonic wedges that evolve from sedimentary prisms with different initial tapers. For the same displacement in the back of the wedge, a sedimentary prism with high initial taper will need less internal deformation than one with low initial taper to reach the critical state. In a low taper sedimentary prism much of the displacement in the back of the wedge will be used to build wedge taper and the wedge will therefore undergo very little translation on the sole fault or basal decollement [11, 30]. A high taper prism, on the other hand, will reach critical taper with a small displacement and the remaining displacement will cause the wedge to slide along its base [11, 30].

Passive margin settings, obtained by restoring balanced cross-sections, typically show variations in the underlying basement slope from the continental shelf to the continental slope [1, 11]. Sedimentary prisms formed in such settings reflect this variation by a change in geometry at the “shelf–miogeocline hinge” from a thinner, lower taper shelf sedimentary prism to a thicker, higher taper migeoclinal prism. Thus, as deformation in an FTB typically progresses from the miogeocline to the shelf (foreland) different parts of the sedimentary prism require different amounts of internal shortening and thickening to reach critical taper [11, 30]. The thicker, higher taper miogeoclinal portion of the prism typically forms one or two dominant thrust sheets that require little or no internal shortening to reach critical taper and therefore undergo large translations. Thrust sheets formed from the shelf part of the prism, at a later stage of thrusting, require significantly more internal shortening to reach critical taper and generally develop many more thrusts with less translation along those thrusts [11].

The internal shortening of any individual thrust sheet can take place by a variety of different deformation mechanisms depending on the ambient deformation conditions (Figure 1). During thrusting, the upper part of the wedge is in the elastico-frictional (EF) regime [31] and will deform by faulting (with cataclasite-development) and flexural-slip folding at various scales [32], and by mesoscopic block-controlled cataclastic flow [3, 32]. At deeper levels within the wedge, below the EF-QP transition, the rocks will deform by quasi-plastic (QP) processes [31] and will develop tight folds and penetrative cleavage [32], together with mylonite development along small to large shear zones (faults) [20, 31]. In addition, variations in rheology and degree of lithification can also promote tight to recumbent

folding even in the shallow parts of accretionary prisms, resulting in diffuse strain distribution without major fault localization [33]. We should note, however, that irrespective of the actual distribution of deformation mechanisms the total energy expended in the emplacement of a large thrust sheet is approximately the same in different areas [3], although the work may be partitioned differently in different settings.

The actual depth at which transition occurs from EF to QP processes is temperature-dependent and will vary with the geothermal gradient. In the simplest case, with a constant geothermal gradient and the same lithotectonic compositions within the wedge, a thinner sedimentary prism (Figure 2a) will have a larger fraction deforming in the EF regime than a thicker sedimentary prism (Figure 2b). Interestingly, this will hold true even after both prisms have reached critical taper (Figure 2a,b). If, on the other hand, we compare sedimentary prisms with the same initial taper but different lithotectonic configurations (Figure 2b,c), it is the material properties of the rocks that will determine the deformation behavior of the wedge. Other factors being equal, a wedge made up of rocks with higher strength will generally have its EF-QP transition at a deeper level than a weaker wedge (compare Figure 2c with 2b). In addition, since it requires less thickening to maintain critical taper, a larger portion of a strong wedge will continue to deform in the EF regime during progressive deformation.

The temperature necessary for the transition from EF to QP deformation is material dependent and will therefore vary from one lithology to another. Thus, for the same geothermal gradient, a carbonate rich wedge will switch from cataclastic behavior to plastic behavior at a significantly shallower depth than a wedge made up dominantly of quartz-rich rocks or quartzo-feldspathic rocks [11]. For an individual wedge of variable lithology, the deformation at a certain depth (and, therefore, temperature) may take place by cataclasis in some lithologies and plastic deformation in others; thus, the switch from EF to QP behavior of the wedge as a whole may be determined by the dominant lithology within the wedge. It is also important to note that since sedimentary prisms do not have a single uniform composition the strength of any wedge as a whole will depend on its overall lithotectonic composition. These factors, together with subtle variations in initial taper and thickness variations within a wedge, will determine how the wedge evolves during progressive deformation.

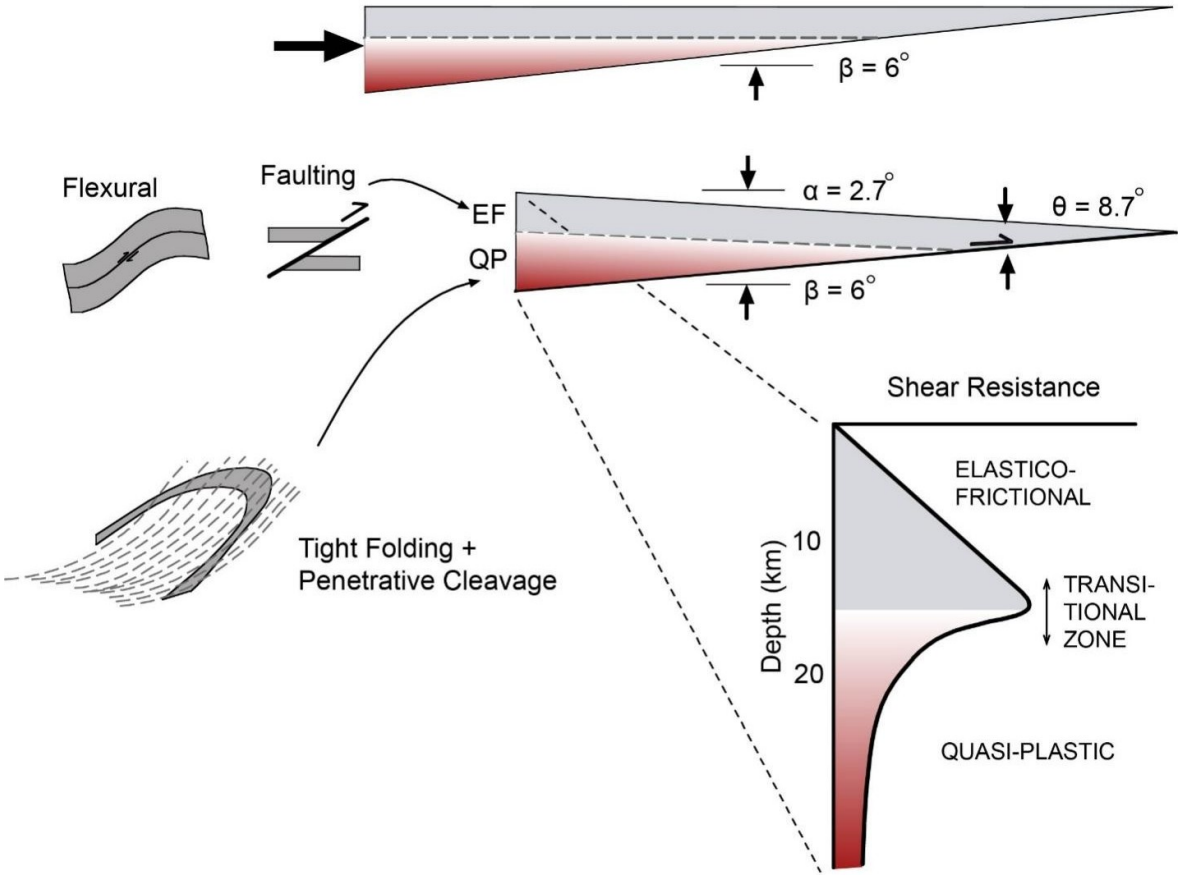

Figure 1. During the evolution of any FTB wedge different parts of the wedge deform by different deformation mechanisms. In the EF regime much of the shortening takes place by flexural slip folding, small scale faulting, and cataclastic flow. In the QP regime the shortening takes place dominantly by tight folding and the development of penetrative cleavage fabrics. The change takes place at the EF-QP transition whose depth is dependent on a variety of factors including the geothermal gradient, dominant lithologies, rates of deformation, and presence or absence of fluids.

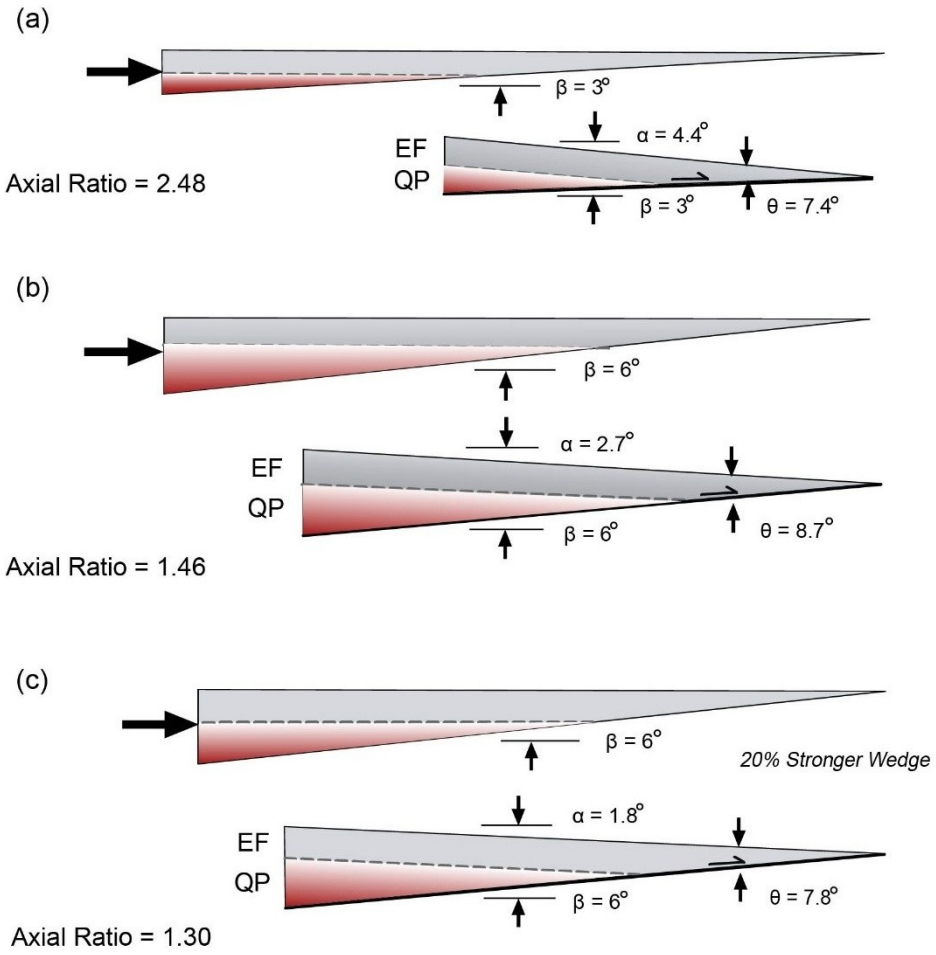

Figure 2. The effects of initial basin geometry on the taper evolution of an FTB wedge. Sedimentary basins with initial basal slopes of (**a**) 3° and (**b**) 6° require different amounts of shortening to reach critical taper. Because α and β have different effects on the criticality of a wedge, the actual critical taper angle is different in the two cases. Also, assuming the same depth to the EF-QP transition (i.e. same geothermal gradient) in the two cases a larger fraction of the low basal slope wedge deforms in the EF regime throughout its deformation history. (**c**) A wedge with dominant lithologies that have higher strength will typically show EF-QP transition at deeper levels than a wedge dominated by weak rocks like "b". The stronger wedge also requires a lesser taper to reach critical state. For initial sedimentary prisms of the same basal slope the stronger wedge will require lesser shortening to reach critical taper, and a larger fraction of the wedge will undergo this deformation by cataclastic processes above the EF-QP transition.

2.3. Changing Conditions during Wedge Evolution

During the progressive deformation of an FTB wedge its structural geometry changes, thereby altering the conditions of deformation. This is particularly important in dominant internal thrust sheets that have prolonged deformation histories and account for most of the shortening that takes place in an FTB wedge [2, 11]. Subtle differences in initial taper, lithotectonic configuration, geothermal gradient, and rates of deformation and erosion, can cause internal thrust sheets in adjoining portions of FTBs to behave quite differently from one another.

In order to evaluate the structural evolution of internal sheets it is best to start with a simple model of thrust sheet emplacement and erosion. When a thick internal (hinterland) thrust sheet first starts to deform, the rocks close to the fault undergo layer parallel shortening (LPS) and fault-parallel shearing [3, 34, 35] under quasi-plastic conditions and develop penetrative plastic deformation fabrics (Figure 3a). As the sheet climbs section over regional-scale ramps and is emplaced on to an upper flat of younger forelandward rocks, it dramatically changes the taper of the rear of the wedge making it locally supercritical (Figure 3b) [11]. The wedge as a whole is now critical and new thrusts can develop and propagate toward the foreland [11]. During the emplacement of such a dominant internal thrust sheet, the sheet carries its own geothermal gradient with it so that the rocks in the hanging wall close to the fault continue to deform under plastic deformation conditions (Figure 3b); at the same time, these hot hanging wall rocks are placed on top of an upper flat of colder footwall rocks, thereby perturbing the geothermal gradient of the wedge as a whole [36]. The higher elevation in the rear wedge enhances erosion there while the

overall supercritical wedge taper induces imbrication at the wedge-toe; these two processes together help to reduce the overall taper of the wedge. As erosion catches up with deformation over time the overall taper of the wedge is reduced to a critical or even sub-critical state so that forward imbrication stops [6]. Concomitantly, the geotherm within the wedge equilibrates, although this happens over a somewhat longer time-frame [36].

For continued wedge advance the rear of the wedge must undergo further deformation to enhance overall wedge taper. Once the geotherm has equilibrated, the rocks of the dominant internal sheet above the upper flat are now in the EF regime (Figure 3c) and any further deformation of the sheet is dominated by cataclasis and flexural slip folding. The resulting overprinting of plastic deformation fabrics by cataclastic features is generally well preserved in FTBs. This is because, under the low pressure-temperature conditions typical of even the internal portions of FTBs, the rocks preserve all of the evidence for successive phases of deformation and earlier deformation features are not obliterated by recrystallization. In other words, the rocks have excellent memory and yield information regarding successive steps in their kinematic and thermal history.

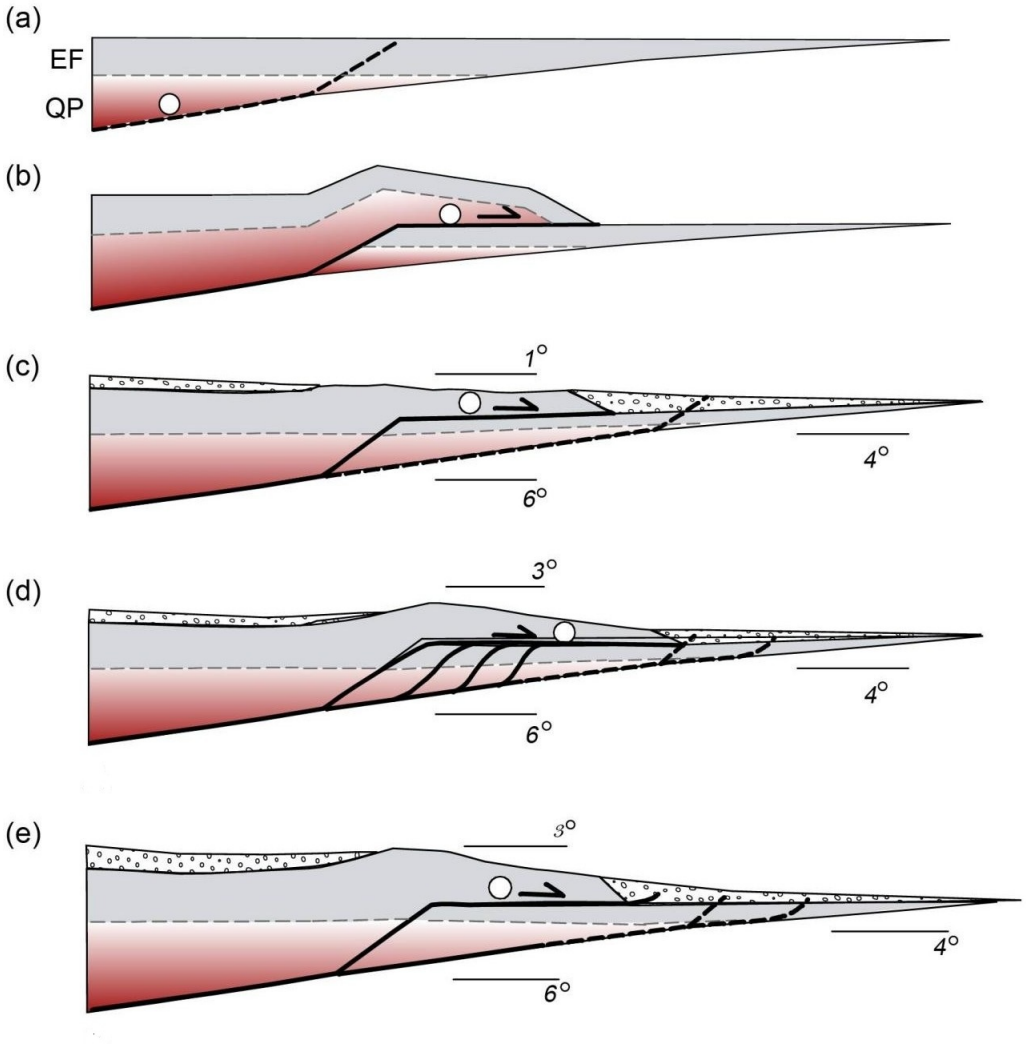

Figure 3. Model for emplacement of a dominant internal thrust sheet. (**a**) Hanging wall rocks (open circle) are initially deformed in the QP regime. (**b**) As the sheet is carried up over a regional-scale ramp it dramatically enhances the overall taper of the wedge. The sheet carries its own geothermal gradient and EF-QP transition, placing hotter rocks in the hanging wall against colder rocks in the footwall along the upper flat; the hanging wall rocks (open circle) continue to deform in the QP regime. (**c**) Over a period of time the geotherm equilibrates and erosion reduces the taper of the wedge. The hanging wall rocks (open circle) are now in the EF regime and any further deformation takes by cataclastic processes. (**d**) Wedge taper can be enhanced by passive uplift and/or translation of the internal dominant sheet by deformation in its footwall (e.g. by duplexing). (**e**) Taper is regained by active deformation of the entire back of the wedge. In this case, much of the hanging wall rocks (open circle) may be deformed by cataclasis in the EF regime, while a large part of the footwall undergoes penetrative deformation in the QP regime.

Depending on the lithotectonic composition of the wedge, continued taper enhancement in the back of the wedge can proceed by one of two possible deformation paths for the dominant sheet. If the dominant sheet is significantly stronger than its footwall it can be passively uplifted and/or translated by deformation (such as duplexing) in its footwall, so that overall wedge-taper increases to the critical state (Figure 3d). Alternatively, if the dominant thrust sheet and its footwall have similar strengths, they can both continue to be actively deformed together by penetrative shortening in the rear of the wedge, thereby enhancing taper of the wedge as a whole (Figure 3e). Either one of these deformation scenarios can be repeated cyclically through time to enhance wedge taper periodically and to allow thrusting to propagate progressively onto the foreland. These are two end-case scenarios but they provide us with models to compare with in testing natural examples.

In what follows, we compare the deformation histories of dominant internal thrust sheets in different segments of the Sevier FTB in Montana and Utah. Our analyses are based on regionally balanced and kinematically restorable cross-sections that incorporate strain data (where available), as well as mesoscopic and microscopic fabric data that help us to constrain the kinematic histories used in our restorations.

3. Geological Examples

The Sevier fold-thrust belt (FTB) is the retroarc FTB of the Cordilleran orogen of North America. It forms the eastern margin of the orogen and is made up of thrust sheets that have been emplaced onto the North American craton (foreland). Along its length the Sevier FTB is broken up into a series of salients or segments [11, 37] that are separated from one another by reentrants that are defined by transverse zones (Figure 4). In the following descriptions we focus our attention on the Lewis salient in NW Montana, and the Provo salient–Central Utah segment in west-central Utah.

3.1. The Lewis Segment

3.1.1. Regional Geology

The Lewis segment of the FTB in NW Montana and southern Alberta is dominated by the Lewis thrust sheet which covers an area of $\sim 45{,}000$ km^2 (Figure 5a). The Lewis thrust trace is ~ 450 km long, extending from Mount Kidd in Alberta [1, 38, 39] to Steamboat Mountain in NW Montana [40]. Near its frontal trace the fault carries a thrust sheet that preserves a stratigraphic sequence made up of 6–7 km of Proterozoic Belt Series rocks and an overlying Paleozoic sequence; the sheet was probably significantly thicker at the time of its emplacement in late Mesozoic time. The Lewis thrust in western Montana has a translation of 100 km or more [41], while just north of the US/Canadian border, refs. [42, 43] place translation of the leading edge of the Lewis thrust sheet, including piggyback motion on eastern footwall sheets, at 140 km. The thrust climbs section from the base of the Proterozoic section to the top of the Mesozoic along a single large ramp, and places Proterozoic rocks in the hanging wall over footwall Mesozoic rocks in the vicinity of Glacier National Park in NW Montana (Figure 5) [17, 41, 44].

The Lewis ramp was reactivated as the Flathead normal fault during post-thrusting extension [41]. This is one of a series of normal faults that have extended the Lewis thrust sheet so that it presently covers a transport-parallel distance of ~ 100 km (Figure 5). As in other parts of the Sevier hinterland, regional restorations must take this extension into account.

3.1.2. Deformation History

The trailing edge of the Lewis thrust sheet shows very little internal deformation. There are small folds and faults, and a weakly developed spaced cleavage is seen in places. The frontal part of the Lewis sheet, exposed in Glacier National Park, has a thick (200–500 m) duplexed fault zone at the base (Figure 6a); examples of these imbricate structures were first noted by Willis [45] at the leading edge of the Lewis in Montana and subsequently mapped by Ross [44] and Ruhle [46] and more recently by Yin [47, 48]. Similar scale structures occur in the Lewis sheet at the Cate Creek and Haig Brook Windows at the NW edge of the Lewis salient [49, 50]. The duplex fault zone developed at various locales perhaps as a response to erosional thinning of the Lewis thrust sheet as it moved up the ramp just west of Glacier/Waterton National Parks. Recent mapping and analysis of structures within the higher parts of the Lewis sheet shows the presence of some faulting (Figure 6a) and folding. In addition, calcareous siltstones and shales in the Proterozoic section show the development of a spaced pressure solution cleavage at acute angles to bedding (Figures 6b,c). The low-angle cleavage (Figure 6b) indicates early layer parallel shortening (LPS) followed by fault-parallel shear.

We have quantified strains in the fine-grained sandstones throughout the Lewis sheet close to our line of cross-section (Figure 5a). Strains were measured parallel to the transport plane (*XZ* plane) using the Fry technique [51–53] and projected onto the line of cross-section (Figure 5b). Strains in the *XY*-plane were also measured in a few samples and show axial ratios close to 1 suggesting that the rocks deformed dominantly by plane strain in the middle of the Lewis salient. The *XZ* strains (parallel to the transport plane) are generally small (axial ratios generally < 1.2) within the sheet and have somewhat higher values (~ 1.3) close to the main thrust (Figure 5b). The lack of penetrative shortening and the paucity of mesoscopic structures (folds, faults) within the Lewis sheet [43, 50], together with the large translation on the Lewis thrust, suggest that the sedimentary prism had significant initial taper, so that most of the tectonic shortening went toward translation of the wedge rather than taper enhancement [6].

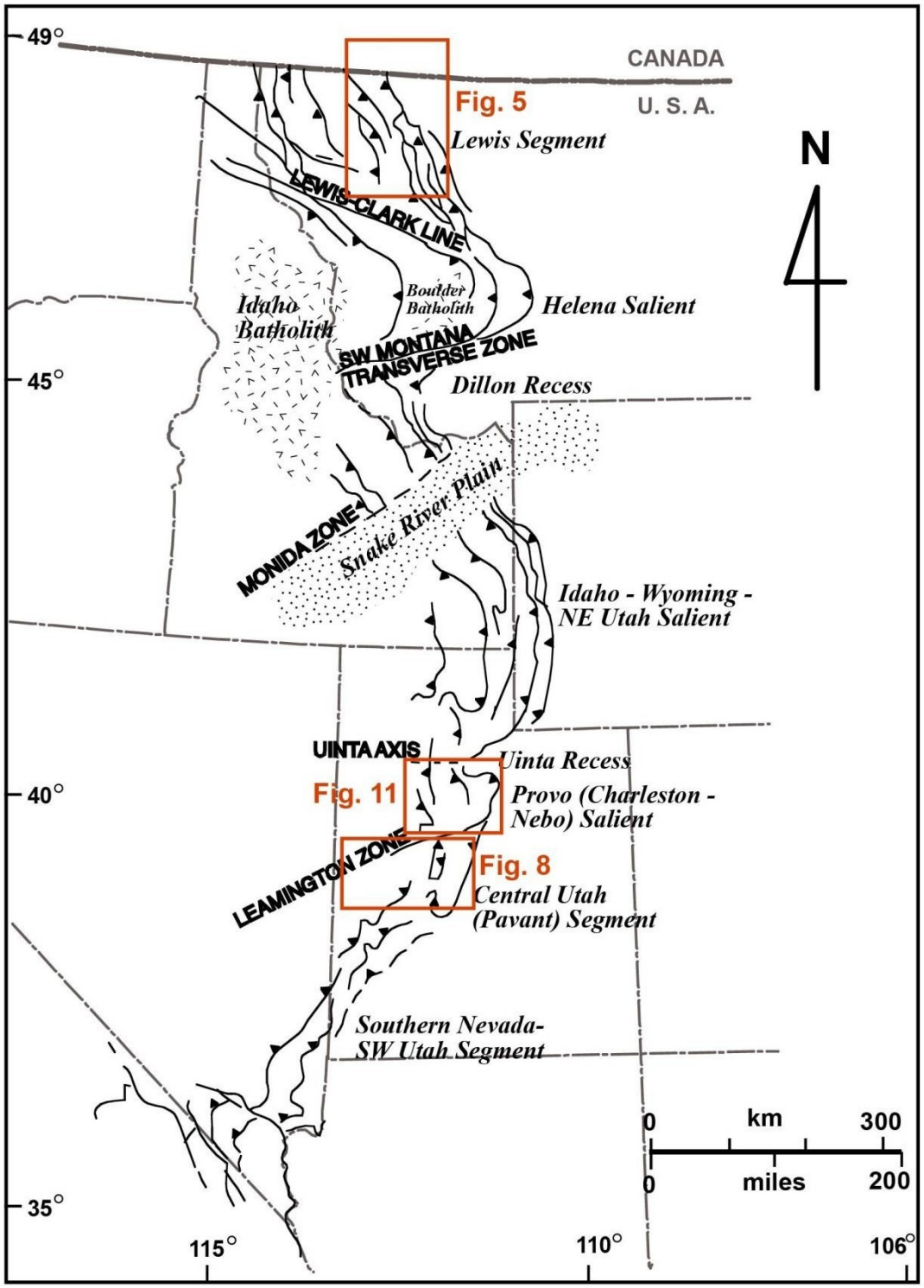

Figure 4. Regional map showing the Sevier fold-thrust belt of the North American Cordillera. The belt is characterized by prominent salients (labeled) that are separated by reentrants located at transverse zones. Boxes indicate areas of detailed maps discussed later in the paper.

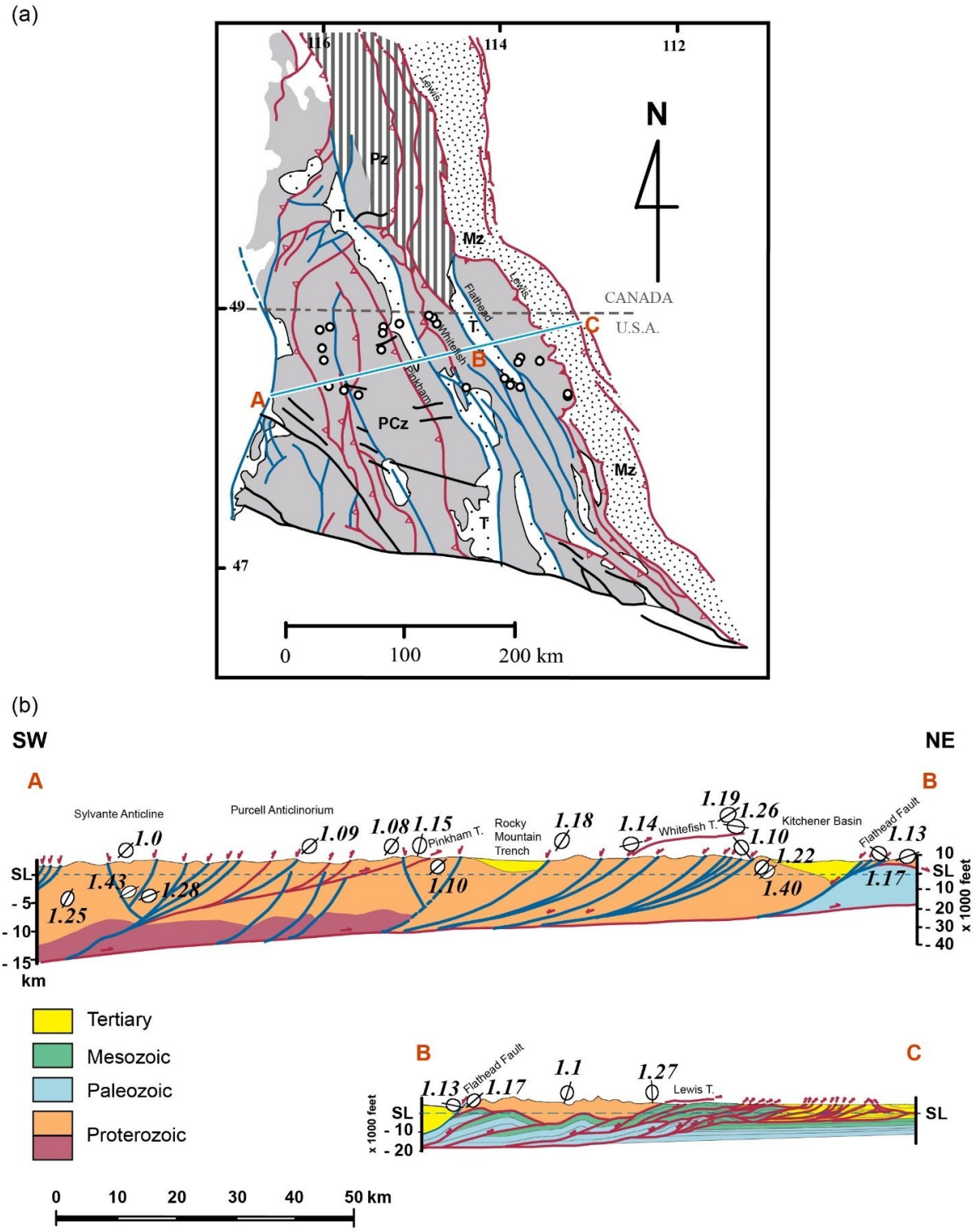

Figure 5. (**a**) Generalized geologic map of the Lewis thrust sheet showing the major thrust faults and stratigraphic sequences. Proterozoic (PCz) and Paleozoic (Pz) rocks are exposed in the hanging wall of the Lewis thrust, and Mesozoic (Mz) rocks in the footwall. Normal faults in the Lewis hanging wall have created half-grabens filled with Tertiary (T) rocks. The line of cross-section and locations for strain measurements (open circles) are also shown. (**b**) Regional cross-section of the Lewis thrust sheet showing major faults and stratigraphic packages; the hanging wall exposes Proterozoic Belt sequence rocks everywhere along this line of cross-section. AB shows the section west of the Flathead normal fault where the Lewis sheet is stripped from Precambrian basement in its footwall, and BC shows the Glacier National Park section with a Paleozoic-Mesozoic duplex in the footwall of the Lewis thrust. Strain axial ratios parallel to the transport plane (*XZ* section) are projected on to the line of section. Note the generally low strain values except near faults.

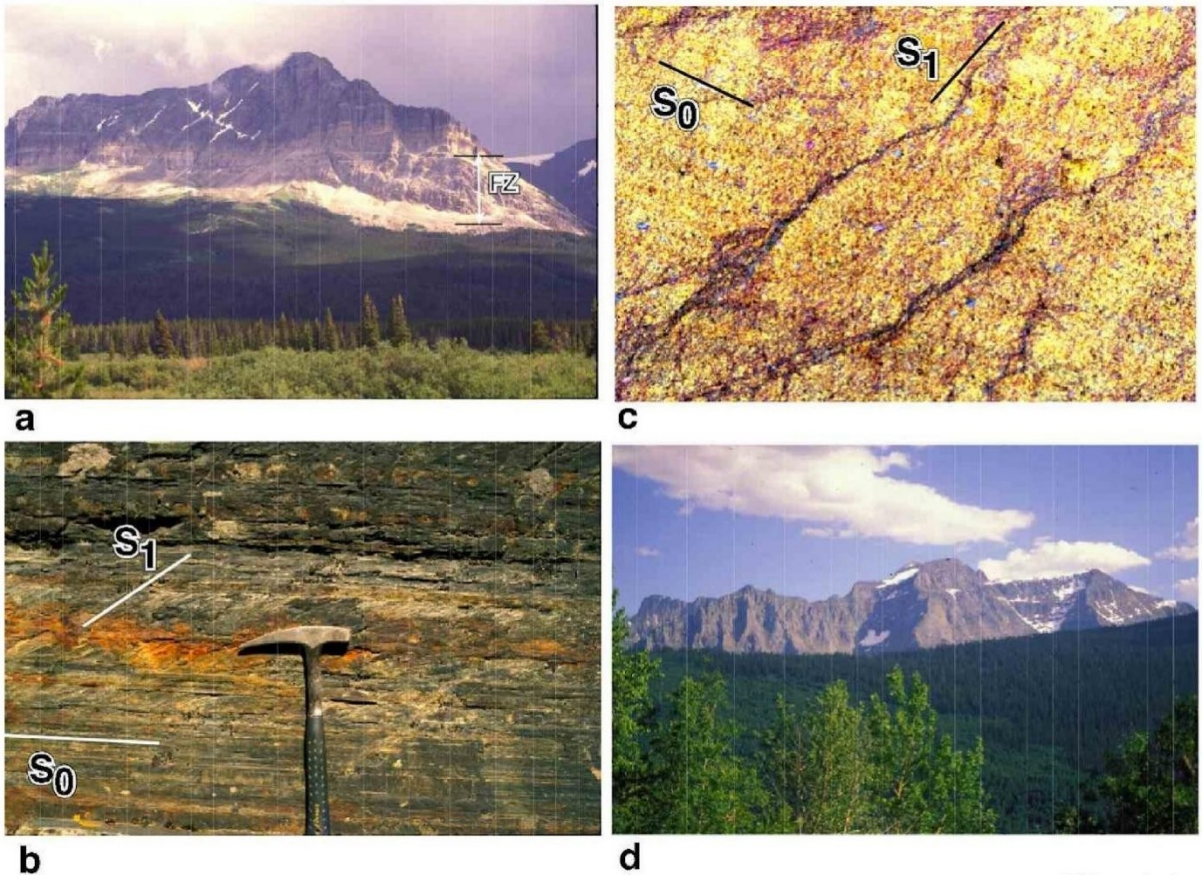

Figure 6. Photographs showing characteristic deformation in the Lewis thrust sheet. (**a**) Exposure of the Lewis thrust sheet in Glacier National Park showing strongly deformed duplex fault zone (FZ) at the base of the section and low-angle wedge faults and higher angle faults/fractures cutting through sub-horizontal beds in the Lewis hanging wall. (**b**) Spaced cleavage (S_1) at low angle to bedding (S_0) in Proterozoic calcareous siltstones in the Lewis sheet. (**c**) Photomicrograph showing spaced and anastomosing pressure solution seams defining cleavage (S_1) at high angle to bedding (S_0) in calcareous siltstone. (**d**) Broad synclinal fold of the Lewis thrust sheet in Glacier National Park. This folding took place during the growth of a duplex in Paleozoic–Mesozoic rocks in the Lewis footwall.

During the late stages of deformation, as thrusting progressed onto the foreland, a sub-thrust duplex developed in the footwall of the Lewis thrust (Figures 5b). The Lewis sheet shows little or no evidence for late-stage internal shortening. Duplexing in the Paleozoic–Mesozoic footwall section *passively* uplifted and broadly folded (Figure 6d) the frontal portion of the Lewis sheet [17]. This helped maintain taper in the frontal portion of the FTB and allowed forelandward propagation of thrusting in the Paleozoic–Mesozoic sequence.

3.1.3. Balanced Cross-Section and Restoration

The regional cross-section (Figure 5b) is drawn along the line of cross-section shown on the map (Figure 5a) and incorporates data from adjoining areas that are projected onto the cross-section. It is similar to earlier published sections [41] but also presents data on penetrative strains in the transport plane. A notable feature of the cross-section is the high density of listric normal faults that have extended the Lewis thrust sheet since the end of contractional deformation. The effects of this extension are removed as a first step in the restoration.

The complex deformation in the footwall of the frontal part of the Lewis sheet makes it necessary to undertake a complex stepwise restoration for these rocks [17]. This restoration is based on structural relationships that are obtained from the southern part of the Lewis salient and the adjoining northern part of the Sawtooth Range [17–19]. The hanging wall of the Lewis thrust, on the other hand, shows very few complexities and is restored in a single step (Figure 7). Because the Lewis sheet has no preserved Paleozoic–Mesozoic section along this line of cross-section, the thicknesses for these units are estimated on the basis of what is known about adjoining areas to the north and south. The geometry of the restored sedimentary prism depends on how far east the Proterozoic basin is assumed to have extended; if the pinchout of the Proterozoic basin is assumed to coincide with that of the Ordovician–Silurian pinchout the restoration yields a sedimentary prism with an initial taper of $10°$–$12°$ (Figure 7b), equivalent to a supercritical taper in a deforming

wedge. Removing the effects of the small amounts of LPS strain (Figure 7a) as a last step in the restoration [54] yields an initial prism with a taper of $8°$–$10°$ (with an average taper of $\sim 9°$) (Figure 7c). Other restored cross-sections (in southern Alberta) that do not account for LPS strain suggest predeformational dips on the sub-Belt/Purcell basement that are higher than $12°$ [42, 43]; this would result in equally large initial sedimentary prism tapers when penetrative strain is removed.

The high initial taper results primarily from the thick Proterozoic Belt sedimentary prism that thins rapidly to the east. This provides us with an explanation of how initial emplacement of the Lewis sheet could have taken place with little or no internal shortening of the sheet. Because the initial prism was already at or close to critical taper it did not need taper enhancement in order for the wedge to start sliding along its base [11]. During the later stages of deformation, wedge taper was enhanced mainly by *passive* uplift of the Lewis sheet over a hinterland dipping duplex in the underlying Paleozoic–Mesozoic section [17]. Contrasting lithotectonic properties of the stronger hanging wall (Lewis sheet) and the weaker footwall (Paleozoic–Mesozoic sequence) may have been instrumental in controlling this deformation.

3.2. The Provo – Central Utah Segments

In the Provo–Central Utah segments of the Sevier FTB (Figure 4) in west-central Utah the internal (hinterland) dominant thrust sheets are the Canyon Range sheet (Figures 8 and 9) and the Sheeprock sheet (Figures 10–12). These sheets have been extensively affected by Tertiary Basin and Range normal faults with very large displacements, so that only small segments of these sheets are exposed in the ranges, separated by basins that are filled with younger sediments. Because the thrust sheets have been deeply eroded the original lateral extents of the thrusts is not very clear, but fragments of these sheets extend as much as 150 km west of their present frontal traces, covering an area of ~ 10000 km^2. The Leamington transverse (oblique) zone separates the two segments (Figure 4) and the geology is dramatically different on either side of the transverse zone. For this reason, we will discuss the two segments separately and then compare them with one another and with the Lewis segment.

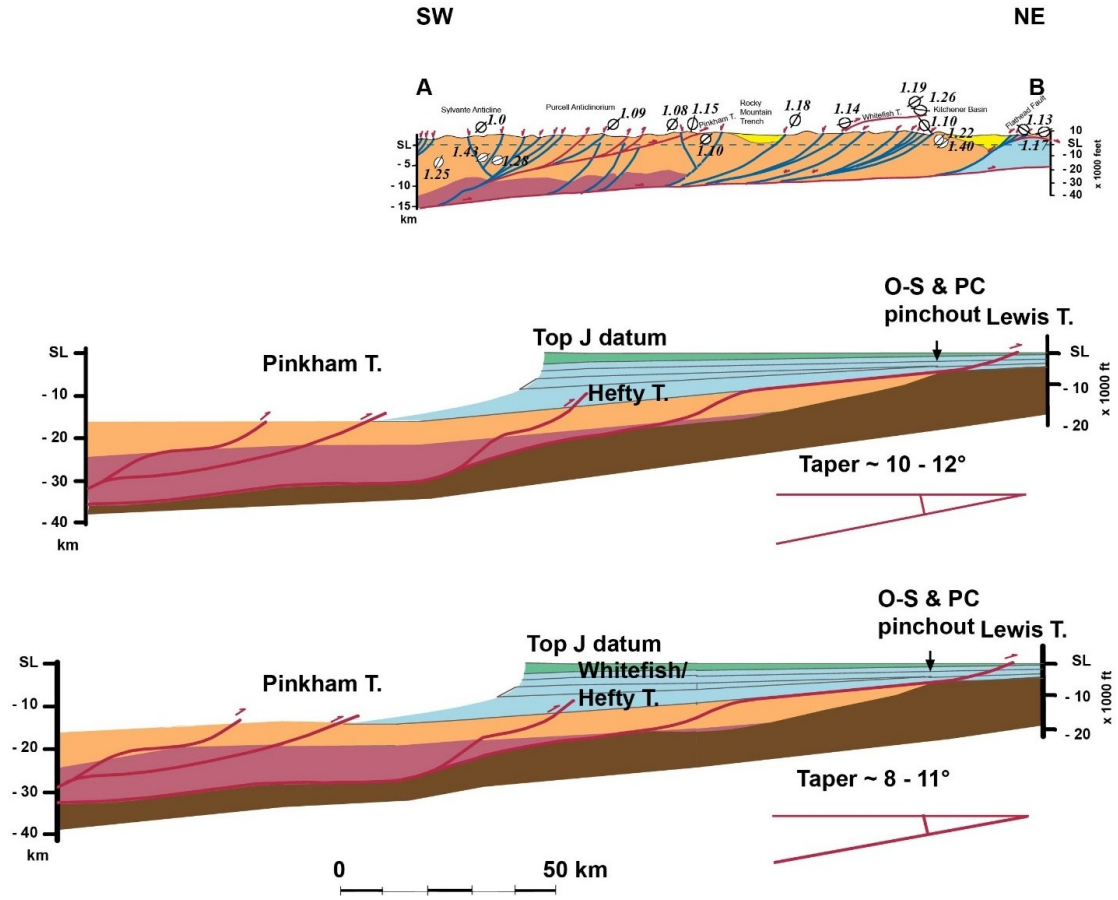

Figure 7. (**a**) Cross-section of the main part of the Lewis thrust sheet west of Glacier National Park showing strain in the Lewis sheet. (**b**) Restoration of the Lewis thrust sheet using estimated thicknesses of Paleozoic and Mesozoic sections based on outcrops in adjoining areas. This is a maximum taper restoration that assumes that the eastern pinch-out of the Proterozoic Belt Basin coincides with the pinch-out of the Ordovician–Silurian sequence in the later Cordilleran Basin. The restored sedimentary prism has an initial taper of $10°$–$12°$. (c) Removing the layer parallel shortening strain from the restoration shown in "b" yields a sedimentary prism with an initial taper of $8°$–$11°$, with an average taper of $9°$.

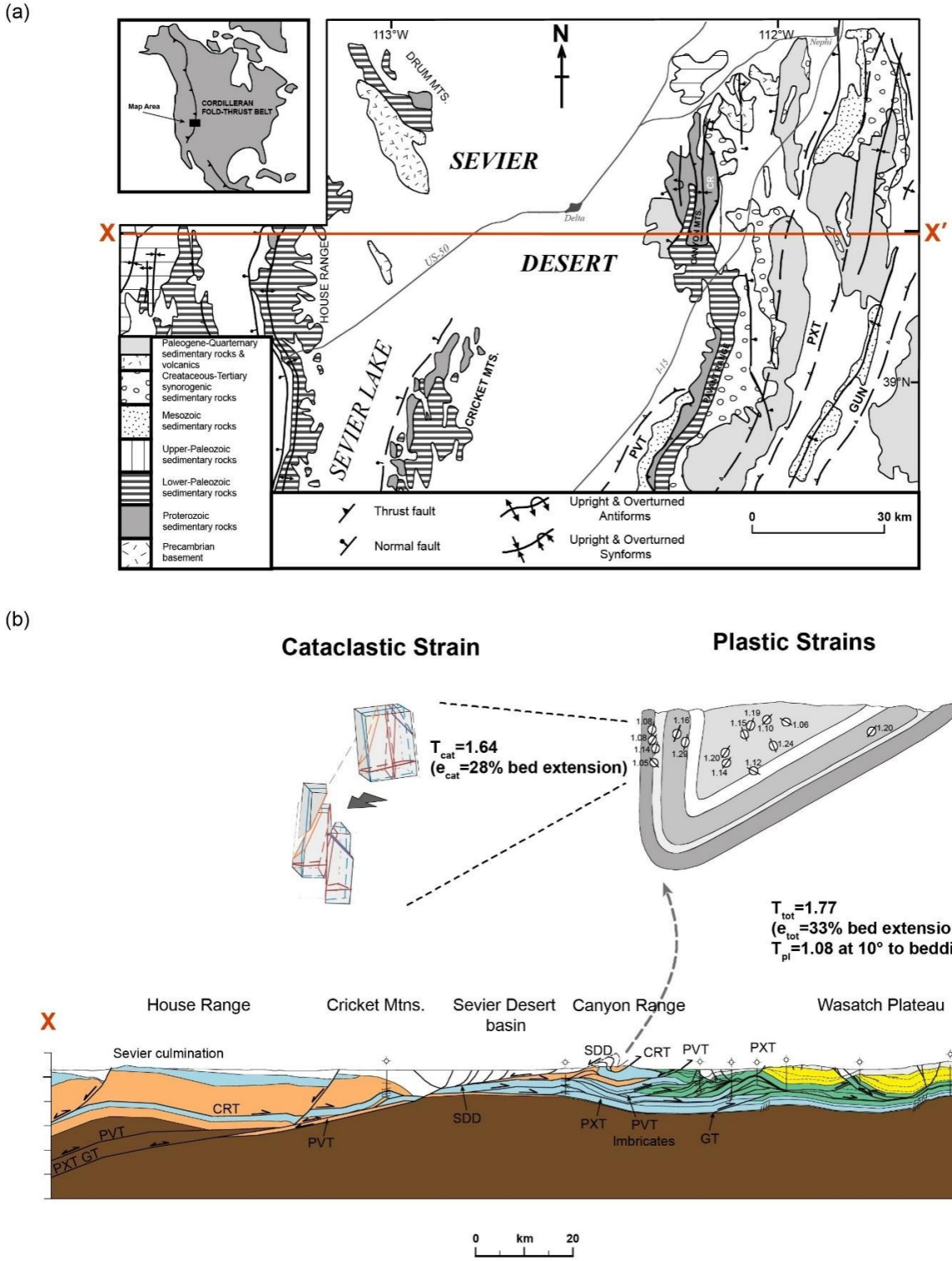

Figure 8. (**a**) Regional geologic map of the Central Utah segment of the Sevier fold-thrust belt showing the major thrust sheets, Canyon Range (CR), Pavant (PVT), Paxton (PXT) and Gunnison (GUN). The thrust sheets have been pulled apart by Basin and Range normal faulting and are only exposed in ranges flanked by Tertiary basins. The line of cross-section XX′ is shown. (**b**) Regional balanced cross-section of the Central Utah Sevier fold-thrust belt (after [55]) showing the major thrust faults. The Sevier Desert Detachment (SDD) is a major low angle normal fault that has strongly affected the dominant internal (Canyon Range and Pavant) thrust sheets. Distribution of plastic strains and estimation of late stage cataclastic strains in the Proterozoic rocks of the Canyon Range sheet are shown (see [56] for details).

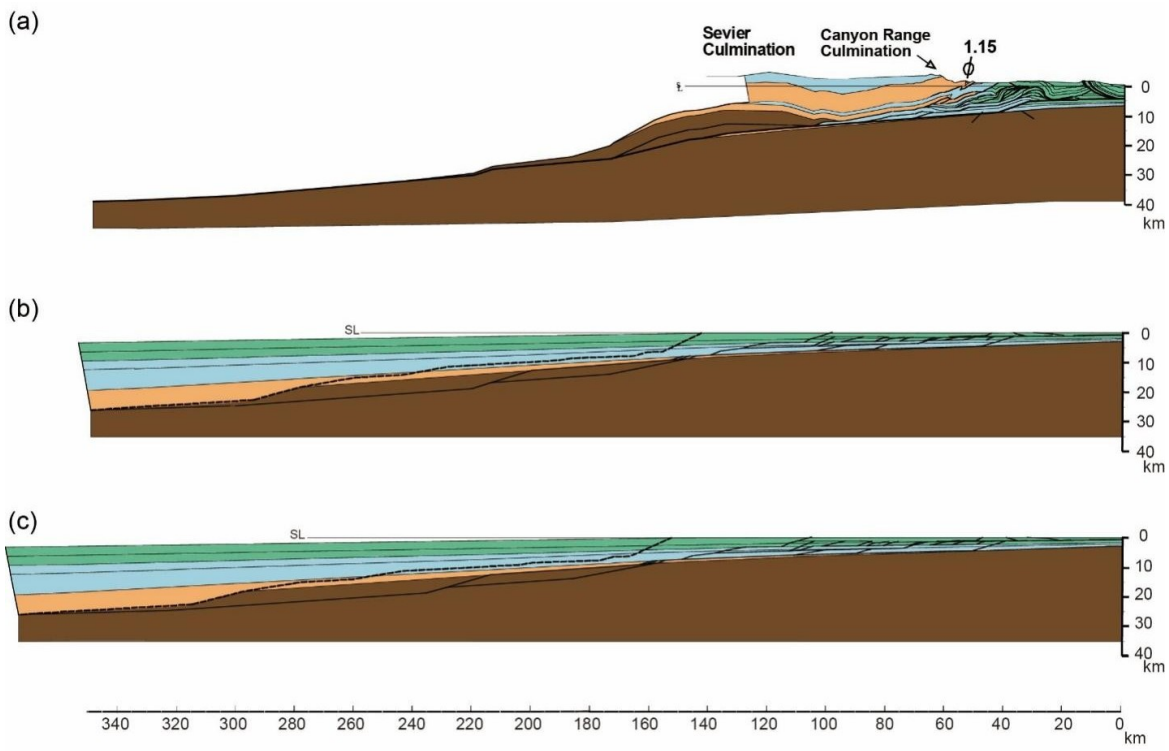

Figure 9. (**a**) Cross-section of the Central Utah segment of the Sevier FTB with the effects of normal faulting removed and showing representative LPS strain in the Canyon Range sheet. (**b**) Restored Central Utah segment of the Sevier FTB obtained by stepwise restoration [55]. (**c**) Removing the layer parallel shortening strain from the restoration shown in "b" yields a sedimentary prism with an initial taper of $4°$–$5°$.

3.3. The Central Utah Segment

3.3.1. Regional Geology

In the Central Utah segment of the Sevier FTB the Canyon Range and Pavant thrust sheets are the principal hinterland thrust sheets. The dominant Canyon Range thrust sheet is well exposed in the Canyon Mountains, but it also has fragments exposed west of the Sevier desert in the Drum Mountains, House Range and Confusion Range (Figure 8a) [3, 55].

The Canyon Range (CR) thrust sheet has a 6 km thick section of Proterozoic coarse-grained quartzites, and the trailing edge of the sheet, made up of Proterozoic through Mesozoic rocks may have been as much as 20 km thick [11, 55]. These rocks were translated as much as 110 km along the CR thrust. The thrust ramped up through the Proterozoic–Paleozoic section in the vicinity of the miogeocline–shelf transition and placed Proterozoic quartzites in the hanging wall on Upper Paleozoic rocks in the footwall [3, 55].

3.3.2. Deformation History

The trailing edge of the CR thrust sheet (exposed in the House Range and Drum Mountains of western Utah) (Figure 8a) shows only moderate mesoscopic deformation, but the Proterozoic quartzites closer to the thrust show a weak but persistent cleavage formed dominantly by plastic deformation processes. At its leading edge the CR sheet, exposed in the Canyon Mountains, shows a somewhat stronger cleavage in quartzites close to the CR thrust and recognizable grain-scale deformation fabrics further up within the sheet [3]. There are also well-developed mesoscopic asymmetric folds in the thin bedded quartzites and wedge faults in somewhat thicker bedded units [3, 56].

Penetrative grain-scale strains were measured in the quartzites using the Fry technique [51–53]. Strain axial ratios parallel to the transport plane (*XZ* plane) are generally small (axial ratios ~ 1.2) and strain ellipses fan around the tight CR syncline hinge (Figure 8b) [3, 32] indicating that most of the penetrative strain is early LPS. There is little or no strain in the *XY* plane (parallel to regional strike) indicating mainly plane strain in the middle of the Central Utah segment. The low values of early LPS strain suggest that wedge taper did not have to be significantly enhanced for translation of the wedge along its base. The overall higher strength of the coarse-grained metamorphosed quartzite wedge in this part of the Sevier hinterland may have facilitated translation at low taper angles [11].

The leading edge of the CR thrust sheet shows strong deformation during the late stages of thrusting. The CR thrust is folded into a tight antiform–synform pair (Figure 10a) with a footwall connecting splay antiformal stack duplex developed in the core of the anticline [15]. Most of the strong deformation in both the hanging wall and the footwall of the CR thrust was accomplished by block-controlled cataclastic flow [3, 32] (Figure 10b), indicating

deformation in the EF regime; this deformation resulted in locally high strains particularly in the common overturned limb of the CR folds that was strongly stretched and thinned (Figure 8b). The footwall duplex shows microstructural evidence for a transition from mainly plastic deformation in the older, higher horses to mainly cataclastic deformation in the younger, lower horses [15]; the older, higher horses were passively uplifted as successive lower horses were emplaced. We interpret this to indicate that this late-stage deformation occurred after the CR sheet had been emplaced over the miogeocline–shelf ramp onto the upper flat, and deformation continued over a period of time while the rocks were progressively unroofed by erosion and the geotherm equilibrated within the wedge.

We note that both the hanging wall and the footwall of the CR thrust underwent deformation by mesoscopic block-controlled cataclastic flow (Figure 10b) during the late stages of thrusting in this part of the Sevier FTB. The shortening and thickening of both the CR hanging wall and the footwall by these processes (in the EF regime) enhanced overall wedge taper in the sedimentary sequence extending from the miogeocline-shelf hinge toward the foreland. In other words, both the hanging wall and footwall of the dominant thrust sheet were *actively* undergoing shortening and thickening during the late stages of FTB development. This created the wedge-taper conditions that allowed thrusting to propagate forelandward into the Paleozoic–Mesozoic sequence on the shelf, as far east as the west limb of San Rafael swell (a foreland Laramide structure) [57, 58].

3.3.3. Regional Cross-Sections and Restorations

A regional balanced cross-section (Figure 8b) [3, 11, 55] is drawn along the line of section shown on Figure 8a. The section presented here is based mainly on a recently published section [55] that incorporates surface geology [3, 13–15, 59–61], seismic data [62, 63] and well data [63, 64]. Our section also includes data on penetrative strains in the transport plane [3, 56]. A feature of the cross-section is the interpretation of the low angle Sevier Desert seismic reflector [62] as a regional-scale listric normal fault [11, 55, 62] that has pulled apart earlier Sevier FTB contractional structures; the effects of this extension are removed as a first step in the restoration (Figure 9).

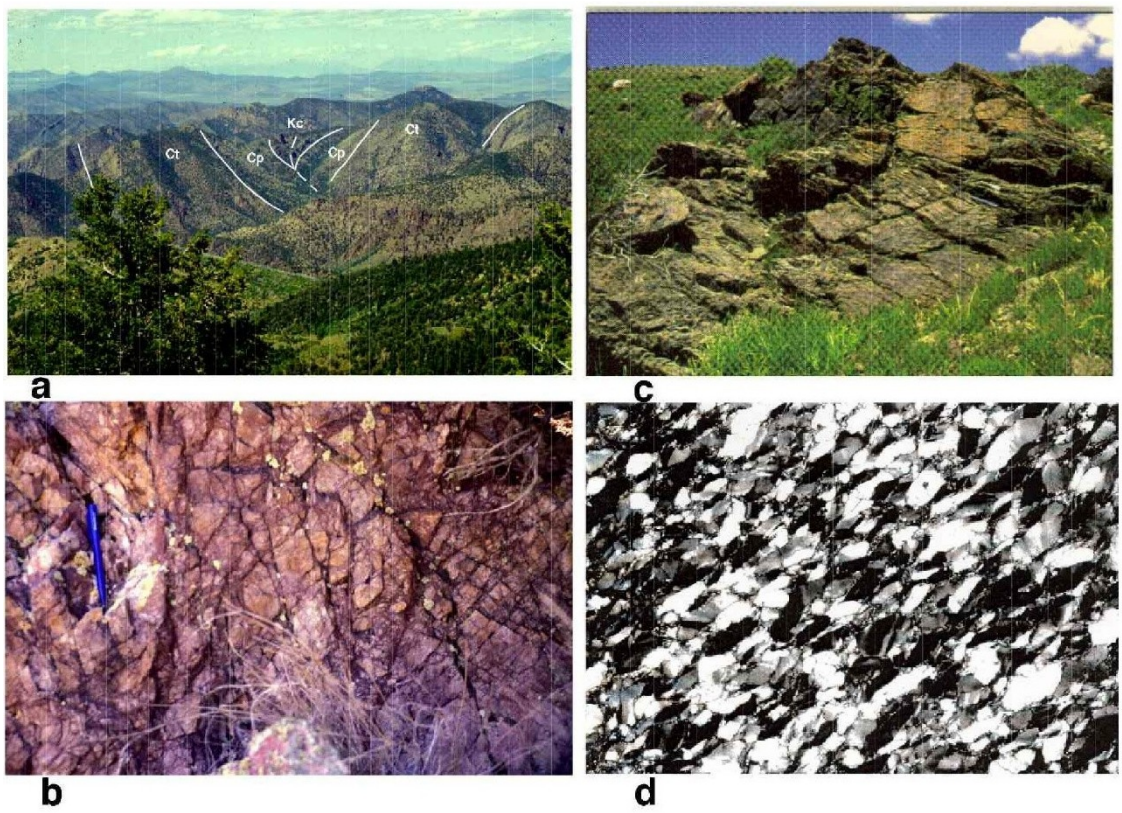

Figure 10. Photographs showing deformation characteristics in the Canyon Range and Sheeprock thrust sheets. (**a**) Photo looking north showing the core of the tight Canyon Range syncline that exposes folded Eocambrian quartzites (Ct), Cambrian shales (Cp), and Cretaceous conglomerates (Kc); the east limb dips $\sim 40^{\circ}$ while the west limb has variable dips ($\sim 50^{\circ}$ to near vertical) and is very strongly deformed. (**b**) Outcrop scale fracturing of Proterozoic quartzites in the Canyon Range syncline; cataclastic flow, with the blocks sliding past each other, results in significant strains. (**c**) Outcrop scale folding and cleavage development in Proterozoic micaceous quartzites in the Sheeprock thrust sheet; note the fanning of cleavage around the fold hinge. (**d**) Photomicrograph of Proterozoic quartzite from the Sheeprock thrust sheet showing a penetrative tectonic foliation defined by parallel alignment of stretched quartz grains and micas.

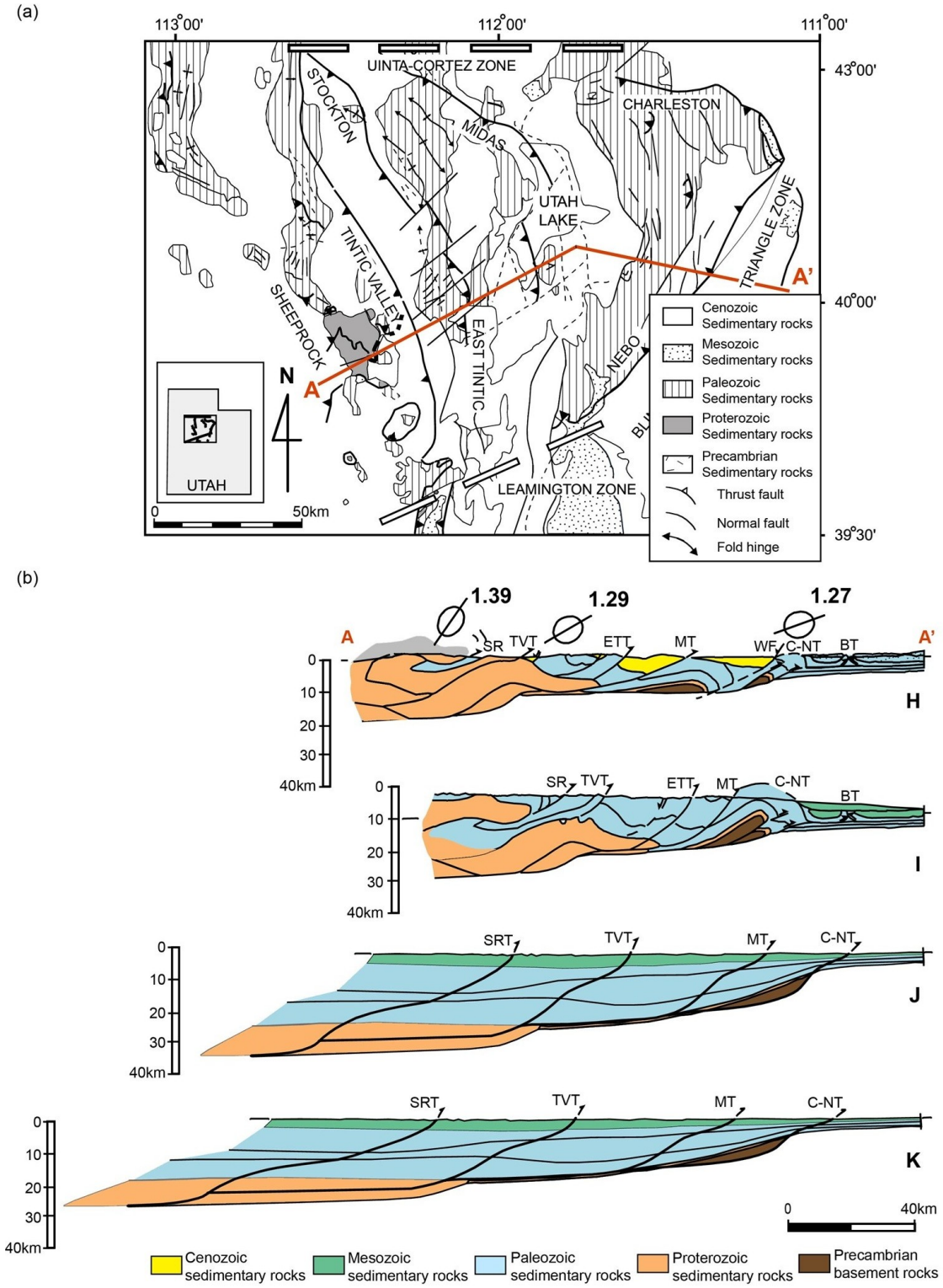

Figure 11. (**a**) Regional geologic map of the Provo salient of the Sevier fold-thrust belt showing the major thrust sheets, Sheeprock, Tintic Valley, East Tintic, Midas and Charleston-Nebo. The thrust sheets have been pulled apart by Basin and Range normal faulting and are only exposed in ranges flanked by Tertiary basins. The line of cross-section AA' has a bend in it in keeping with the local tectonic transport direction. (**b**) AA'. Regional balanced cross-section of the Provo salient in the Sevier fold-thrust belt (after [11]) showing the major thrust faults. Representative LPS strain measurement in the different thrust sheets are shown (see [65] for details). I. Cross-section of the Provo segment of the Sevier FTB with the effects of normal faulting removed. J. Restored section obtained by stepwise restoration of successive thrusts [11]. K. Removing the layer parallel shortening strain from the restoration shown in "c" yields a sedimentary prism with an initial taper of $\sim 10^{\circ}$ near the miogeocline-shelf hinge, and a taper of $< 3.5^{\circ}$ at the back of the wedge.

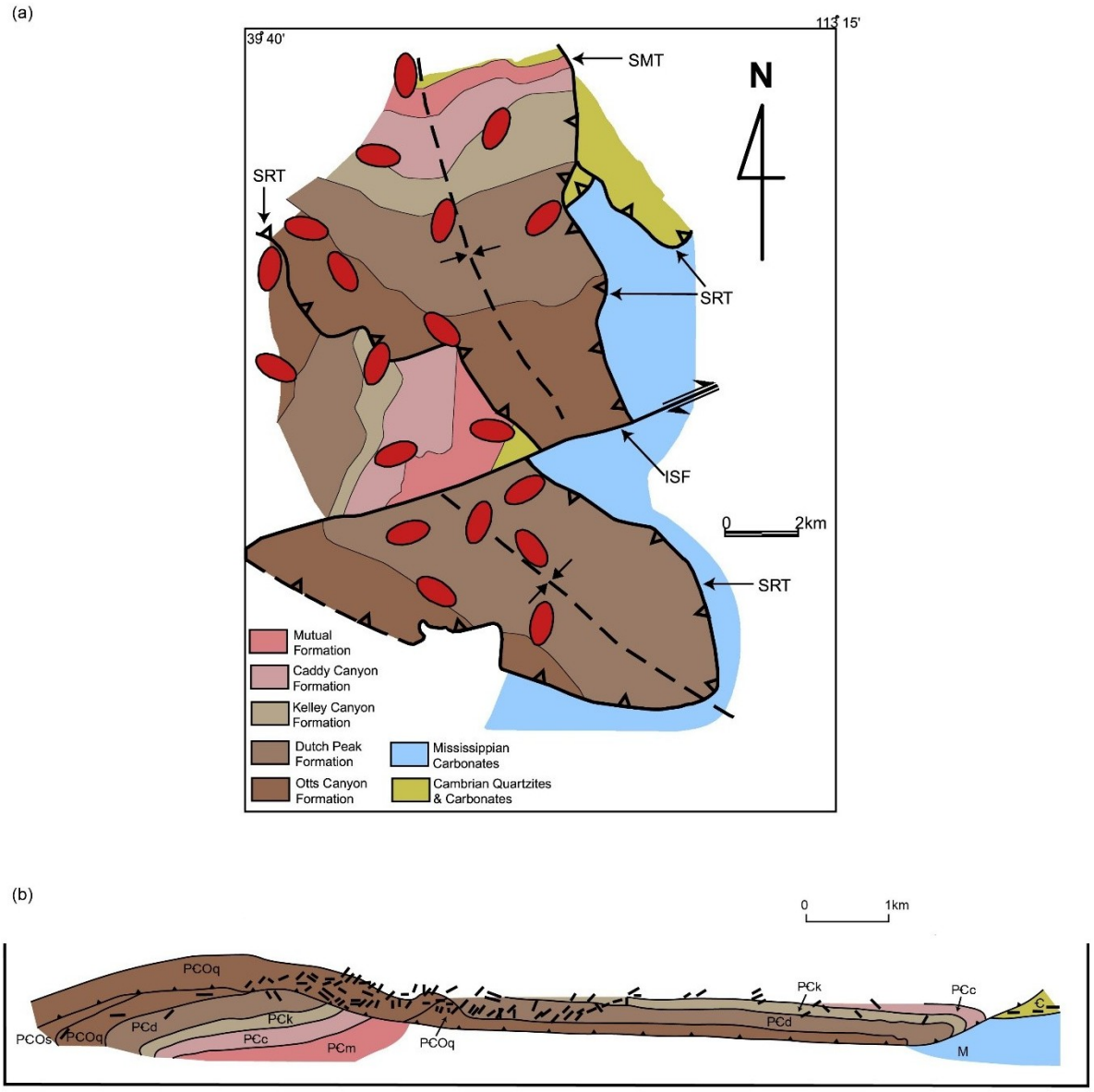

Figure 12. (**a**) Geologic map of the Sheeprock mountains showing the broadly folded Proterozoic–Paleozoic sequence of the Sheeprock thrust sheet. Representative strain ellipses show variation in stretching direction within the sheet with an overall radial stretching pattern; this is overprinted by prominent pure shear flattening in the back-limb of the syncline resulting in transport-perpendicular stretching directions. (**b**) Cross-section showing the broad synclinal folding of the Sheeprock thrust sheet, and the general pattern of acute cleavage-bedding angles throughout the sheet.

Multiple reactivation of the internal thrust faults and a complex deformation history [3, 11, 15] make it necessary to undertake a careful stepwise restoration to ensure that successive steps in the restoration are kinematically feasible; the details of the stepwise restoration of successive thrusts are described by [55]. Because Upper Paleozoic and Mesozoic rocks are eroded and no longer preserved in the Sevier hinterland [59] their thicknesses have to be estimated on the basis of isopach gradients. The geometry of the restored sedimentary prism [55] has a taper of $5°$–$6°$. Removing the effects of the small amounts of LPS strain reduces the initial taper to $4°$–$5°$.

In spite of a thick Proterozoic through Mesozoic section in the hinterland the initial sedimentary prism has only a moderate taper of $4°$–$5°$. This is because the change in thickness of the sedimentary section takes place gradually over a long distance. The dominance of coarse-grained recrystallized quartzites in the Proterozoic section and the incorporation of crystalline basement slices in the hanging wall during thrusting gave the wedge high strength and increased its taper so that it required limited taper enhancement in the sedimentary section before the large internal thrust sheets were emplaced (Figure 2). During the later stages of deformation taper enhancement in the hinterland was achieved by *active* shortening and thickening in both the hanging wall and the footwall of internal thrusts mainly by cataclastic processes [3, 56].

3.4. Provo Segment

3.4.1. Regional Geology

In the Provo segment of the Sevier FTB the Sheeprock thrust sheet is the dominant thrust sheet (Figure 11a). This sheet has a thicker ($\sim$10 km) Proterozoic section than the Canyon Range sheet in the Central Utah segment and is made up mainly of siliciclastic rocks [54, 66, 67]. The trailing edge of the Sheeprock sheet may have carried a Proterozoic through Mesozoic section that was as much as 25 km thick (Figure 11b) [11]. The thrust sheet was translated through only $\sim$10 km but the rocks show map-scale overturned folding in both the hanging wall and the footwall suggestive of large-scale fault propagation folding. The Sheeprock thrust ramped up through the Proterozoic – Lower Paleozoic section placing Proterozoic hanging wall rocks on Lower Paleozoic footwall rocks.

3.4.2. Deformation History

The leading edge of the Sheeprock thrust sheet in the Sheeprock Mountains exposes Proteozoic and Lower Paleozoic rocks that are folded into a broad syncline together with the underlying thrust (Figure 12a,b) [54, 67]. The rocks of the thrust sheet show open to tight folding at all scales particularly in thin-bedded units (Figure 10c). In addition, they are penetratively deformed, with well-developed cleavage formed dominantly by plastic deformation processes (Figure 10d) [54, 67]. Fanning of cleavage around mesoscopic folds (Figure 10c) indicates that the cleavage fabric formed by early LPS before the beds were folded. At a larger scale the cleavage shows an acute angle relationship to bedding throughout much of the thrust sheet (Figure 12b), indicating modification of the LPS fabric by fault parallel shearing early in the deformation history [67]. The mountain ranges defining the trailing edge of the Sheeprock sheet in western Utah expose mildly deformed Lower to Middle Paleozoic rocks that are extensively intruded by Tertiary igneous rocks [59].

The Proterozoic quartzites in both the hanging wall and the footwall of the Sheeprock thrust are penetratively deformed and the three-dimensional strain in these rocks has been systematically measured and analyzed [54, 67] using the Fry technique [51–53]. Strain axial ratios in the hanging wall parallel to the transport plane (*XZ* plane) range from 2.5 close to the fault to 1.2 high up within the sheet, with an average of 1.5–1.6; footwall *XZ* strain axial ratios range from 1.1 to as high as 1.8 close to the fault [54]. The strain axial ratio and the angle of the strain long axis relative to the shearing plane (parallel to the thrust) at various locations within the thrust sheet indicate that the total penetrative deformation is a result of superposition of inhomogeneous simple shear parallel to the fault and pure shear flattening perpendicular to the fault [54, 68]. This type of deformation can lead to axis switching in the strain ellipsoid as the strains increase, with the long axis switching from transport-parallel to an orientation parallel to strike [69]; the strain axis switching pattern observed on the back-limb of the Sheeprock syncline (Figure 12a) [54] is best explained as resulting from this mechanism. The axis-switching pattern is superposed on an overall radial pattern of transport-parallel long axes at the front of the sheet that is interpreted (based on 3-D finite element modeling) as an effect of 3-D gravitational spreading in the back of the wedge [26]. The large LPS strains suggest that the sedimentary prism had to undergo significant taper enhancement by plastic deformation processes to allow thrusting along a sole thrust, and also explains the small translation observed along the thrust fault.

The overall strain distribution in the Sheeprock hanging wall ranges from flattening to constrictional, with a tendency toward plane strain parallel to the transport plane. However, on a regional scale, the plane strain pattern is only observed in the middle of the Provo salient [26, 65]. Along the northern (Uinta transverse zone) and southern (Leamington oblique zone) margins of the salient the *XZ* strain orientations radiate outward from the regional transport direction, and this pattern is accentuated during the later stages of deformation [65, 70].

During the late stages of deformation, the Sheeprock thrust sheet underwent cataclasis that overprinted all earlier structures and is observable at mesoscopic and microscopic scales [15]. Late stage cataclasis is also seen in the Sheeprock footwall, both in the southern Sheeprock Mountains and in the Tintic Valley thrust sheet in the Gilson Mountains [70]. As in the adjoining Canyon Mountains the late-stage deformation in the Gilson Mountains occurred in the EF regime and was accomplished by block-controlled cataclastic flow [3, 70]. The late-stage deformation shows significant vertical axis rotation of local transport planes along the lateral boundaries of the Provo salient where the thrust sheets were emplaced over regional scale lateral and oblique ramps [70]; this results in a truly three-dimensional strain field for the salient as a whole. Overall thickening of the middle of the salient continued by fault propagation folding and faulting. This continued deformation in the hanging wall and footwall of the Sheeprock thrust resulted in *active* thickening of the entire rear wedge that enhanced overall wedge taper and allowed thrusting to propagate toward the foreland.

3.4.3. Regional Cross-Sections and Restorations

A regional cross-section (Figure 11b) is drawn along the line of section shown on Figure 11a [11]. Because of extensive basin-fill in the normal faulted basins formed during Tertiary Basin and Range extension there is only limited information available from surface geologic maps in this segment of the Sevier FTB. This, together with a paucity of subsurface data, results in a regional cross-section that is only approximately balanced [11]. Significant strains (axial ratios averaging 1.5–1.6) are observed in the internal thrust sheets [65] and are incorporated in the cross-section; the external sheets also show some penetrative deformation (strain axial ratios $\sim$1.28) (Figure 11b-H).

A stepwise kinematically feasible retrodeformation includes removal of late-stage extension as a first step

(Figure 11b-H) [11, 68]. Each of the major thrust sheets involves limited translation along the fault but shows regional scale fault propagation folding extending up through the Proterozoic–Mesozoic section. Each sheet is restored using line-length and area balancing using the basement–cover contact as the detachment depth, since Proterozoic cover rocks are always observed in the hanging walls of these sheets and the basement is not seen (Figure 11b-J). The depth of this contact is estimated by using regional stratigraphic data and return to regional dip arguments.

The final restoration suggests that the sedimentary prism was strongly tapered ($\sim 10^{\circ}$) over a short distance on the outboard side of the miogeocline–shelf hinge, with a steep basement slope. This is consistent with the interpretation of the Provo salient (particularly the strongly convex Charleston–Nebo thrust system) as having evolved from a deep embayment that extended eastward from the main miogeoclinal margin during the Proterozoic and into mid-Paleozoic (Oquirrh) time [65, 71]. Beyond the edge of the miogeocline the sedimentary prism is thick but has a low basal slope and therefore a low taper ($\sim 4^{\circ}$). Removal of the LPS strain as a last step in the retrodeformation (Figure 11b-K) [54] lowers the taper even more (to $\sim 3^{\circ}$).

The low initial taper at the back of the tectonic wedge required significant taper enhancement prior to wedge emplacement along a sole thrust. Since much of the lower part of the wedge was below the EF-QP transition for quartzites much of the shortening and thickening took place by plastic deformation processes, with a dominance of fault propagation folding over translation along thrust faults, and the development of a penetrative cleavage in the Proterozoic quartzites (Figure 11b-K). With little lithotectonic contrast between successive internal thrust sheets they all continued to *actively* shorten and thicken during the later stages of deformation as thrusting propagated onto the foreland. Some of this late-stage deformation in internal sheets took place by cataclasis as the rocks were brought progressively closer to the surface as a result of erosion off the top of the tectonic wedge.

4. Discussion

The internal (hinterland) thrust sheets in different segments of the Sevier FTB show similarities and differences in their deformation patterns. Because of their large size and great displacement, they are clearly dominant in their roles in the evolution of the FTB as a whole within each segment. Lateral variations in initial basin geometry, stratigraphy, lithotectonic characteristics (Figure 13) and geothermal gradient all contribute to the deformation characteristics of the dominant sheets, and this in turn affects the overall evolution of the external segments of the FTB.

In each of the FTB segments described above the dominant internal sheet has the largest displacement of any sheet within that segment and is active through the entire period that FTB deformation takes place [11]. The displacement may be differently partitioned into translation and internal deformation in the different cases. In all cases the dominant sheets are repeatedly reactivated to create higher elevations in the back of the wedge and maintain critical taper within the wedge. Timing information suggests that this is directly instrumental in driving thrusting in the external portion of the FTB [6, 11].

In the Lewis segment the sedimentary prism had sufficient initial taper (Figure 13) to allow the dominant Lewis sheet to be emplaced with little or no internal deformation. Although the rocks at the base of the sheet were initially deformed at depths of ~ 20 km, the lack of plastic deformation features in quartz-rich rocks suggests that deformation took place at very low metamorphic grades; the most likely explanation for this is a low geothermal gradient in this portion of the FTB. During the later stages of deformation there was sufficient lithologic contrast between the quartz-rich Proterozoic Lewis hanging wall rocks and the weaker clay- and carbonate-rich Paleozoic–Mesozoic footwall rocks (Figure 13) for deformation to be confined to the footwall and to allow the Lewis sheet to be uplifted and translated *passively* (Figure 3d).

In the Central Utah segment, by contrast, the sedimentary prism had a lower initial taper even though the back end of the wedge had approximately the same thickness as in the Lewis segment (Figure 13). In spite of the lower taper, the coarse recrystallized quartz-rich rocks that make up the lower third of the wedge (Figure 13) gave the wedge sufficient strength to allow the dominant Canyon Range thrust sheet to be emplaced with very little internal shortening. The quartzites show plastic deformation features indicating higher metamorphic grades than in the Lewis sheet and suggesting a higher geothermal gradient in this FTB segment. In the late stages of thrusting there was very little lithologic contrast between the Canyon Range sheet and its footwall (Figures 9 and 13) and the entire back of the wedge was actively shortened and thickened by cataclastic processes to maintain critical taper (Figure 3e).

The adjoining Provo segment has a thicker sedimentary prism but the hinterland portion had very low initial taper (Figure 13). The wedge required significant shortening and thickening to achieve critical taper. Much of the lower half of the wedge was in the QP regime and deformation in the Proterozoic siliciclastic rocks took place by plastic deformation mechanisms (Figures 10 and 13). Most of the displacement in the back of the wedge was absorbed in penetrative grain-scale deformation and folding (Figure 10c,d) to achieve critical taper, and the dominant Sheeprock thrust shows relatively small translation. As in the case of the Central Utah segment, here too there was little lithologic contrast between the Sheeprock hanging wall and footwall rocks during the late stages of deformation (Figures 11b and 13), and the entire back end of the wedge was *actively* shortened and thickened by plastic deformation in the lower part of the wedge and cataclastic processes closer to the surface; this helped to maintain critical taper in the wedge as a whole as thrusting progressed into the external portions of the FTB.

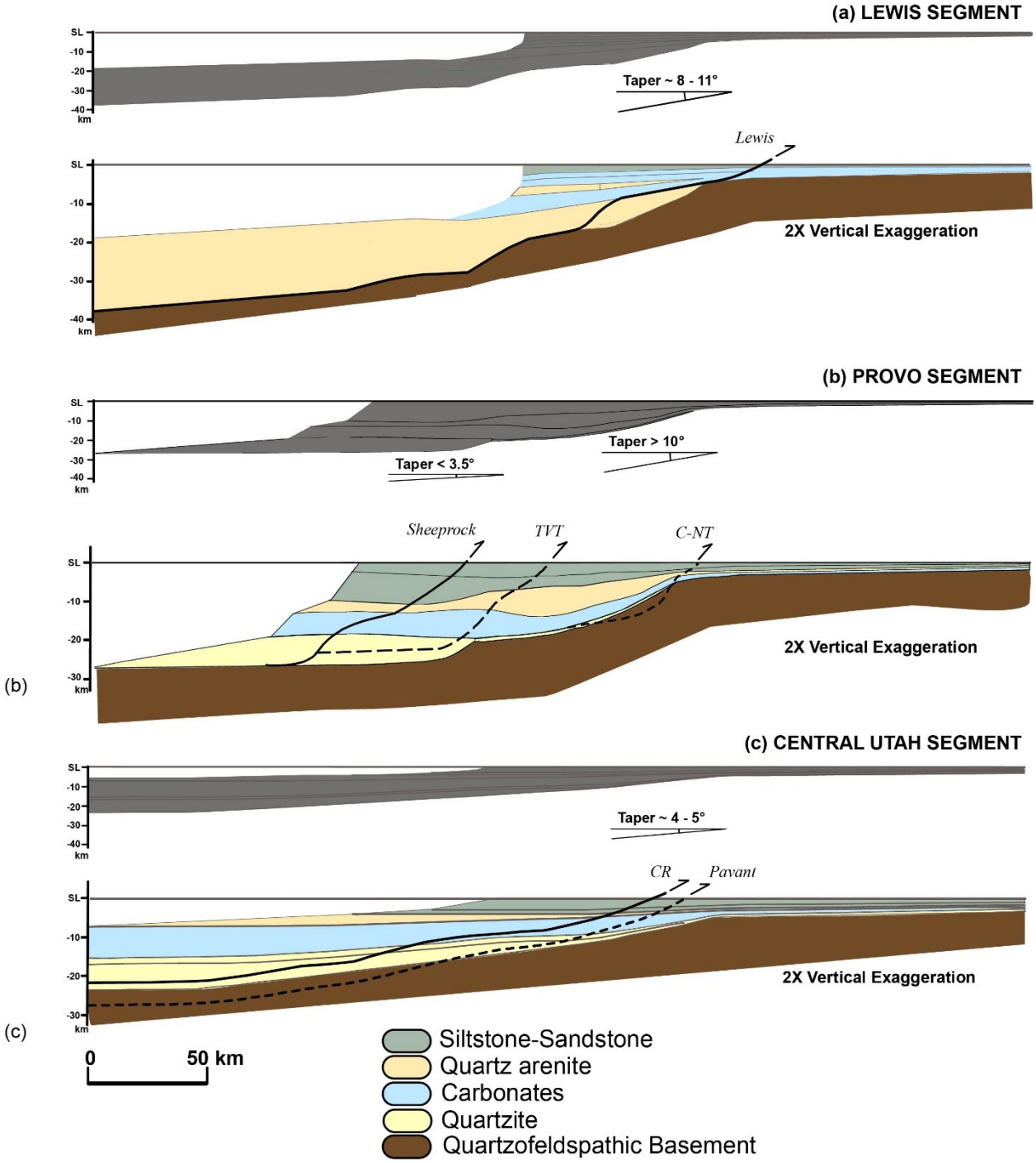

Figure 13. Comparison of lithotectonic configurations and initial tapers of the sedimentary prisms in three segments of the Sevier FTB. For each area the real wedge taper is shown in the grey cross-section (with equal vertical and horizontal scales); the lithotectonic makeup of the wedges are shown in colored cross-sections with 2x vertical exaggeration. In all cases the Proterozoic sections are quartz-rich although there are significant variations in grain-size from one segment to another affecting rock strength. The Paleozoic sections are typically carbonate-rich, although the Middle Paleozoic (Oquirrh) section in the Provo segment is quartz-rich. The Mesozoic sections are dominantly fine-grained clastics. The variations in taper and lithotectonic packaging result in significantly different deformation histories, both during the initial emplacement of the dominant internal thrust sheets and during continued deformation as thrusting progresses toward the foreland (see details described in the text).

5. Conclusions

Studies on internal thrust sheets in different parts of the Sevier FTB allow us to come to the following conclusions about their behavior.

1. Internal (hinterland) thrust sheets are dominant sheets in an FTB in terms of both size and displacement.
2. They tend to be active over the entire period of deformation in an FTB and are instrumental in maintaining critical taper in the FTB wedge as a whole.
3. Some internal sheets (e.g. Lewis sheet of the Lewis segment) are passively uplifted (by footwall deformation) in the late stages of FTB evolution in order to maintain critical taper.
4. Other internal sheets (e.g. Canyon Range sheet of the Central Utah Segment, Sheeprock sheet of the Provo Salient) are actively shortened and thickened in the late stages of FTB evolution to maintain critical taper.
5. The actual behavior of internal sheets are controlled by the combined effects of a number of factors, including initial taper of the sedimentary prism and its lithotectonic makeup, the geothermal gradient, the mechanisms and rates of deformation, and the presence or absence of fluids (that might affect some of the other factors).

Author contributions

G.M.: Conceptualization, Data curation; Writing—original draft. S.E.B.: Data curation, Writing—review and editing. S.K.: Data curation, Writing—review and editing. M.M.: Data curation; Writing—review and editing. Z.I.: Data curation, Writing—review and editing. A.S.: Data curation, Writing—review and editing.

Funding

Funding for this work was provided by NSF grants EAR-9418688, EAR-0208001, and EAR-0001030 to G. Mitra. Additional support was provided by the Petroleum Research Fund, administered by the American Chemical Society, under grants 21954-AC2 and 33387-AC2 to G. Mitra. Summer fieldwork for the various projects was supported by Geological Society of America Penrose Research Grants, Nuria Pequera grants from the University of Rochester, and USGS EDMAP mapping funds through the Utah Geological Survey.

Institutional Review Board Statement

Not applicable.

Informed Consent Statement

Not applicable.

Data Availability Statement

All data are included in this published article, and more details can be provided by the authors upon request.

Acknowledgements

The authors thank the anonymous reviewers and the handling editor for their constructive comments. The authors also gratefully acknowledge the students of the Structural Geology Laboratory at Yonsei University for their assistance in redrawing the figures in color.

Conflicts of Interest

The authors declare that they have no known competing financial interests or personal relationships that could have appeared to influence the work reported in this paper. Corresponding author Sanghoon Kwon is a Co- Editor-in-Chief of this journal and was not involved in the editorial review or the decision to publish this article.

Use of AI and AI-Assisted Technologies

No AI tools were utilized for this paper.

References

1. Price, R.A. Large-scale gravitational flow of supracrustal rocks, southern Canadian Rockies. In *Gravity and Tectonics*; DeJong, K.A., Scholten, R., Eds.; Wiley: New York, NY, USA, 1973; pp. 491–502.
2. Price, R.A. The Cordilleran foreland thrust and fold belt in the southern Canadian Rocky Mountains. In *Thrust and Nappe Tectonics*; McClay, K.R., Price, N.J., Eds.; Geological Society Special Publication 9; The Geological Society of London: London, UK, 1981; pp. 427–448.
3. Ismat, Z.; Mitra, G. Fold-thrust belt evolution expressed in an internal thrust sheet, Sevier orogen: The role of cataclastic flow. *Geol. Soc. Am. Bull.* **2005**, *117*, 764–782. https://doi.org/10.1130/B25514.1
4. Yonkee, W.A. Basement–cover relations, Sevier orogenic belt, Northern Utah. *Geol. Soc. Am. Bull.* **1992**, *104*, 280–302. https://doi.org/10.1130/0016-7606(1992)104<0280:BCRSOB>2.3.CO;2
5. Yonkee, W.A.; Parry, W.T.; Bruhn, R.L. Relations between progressive deformation and fluid–rock interaction during shear-zone growth in a basement-cored thrust sheet, Sevier orogenic belt, Utah. *Am. J. Sci.* **2003**, *303*, 1–59. https://doi.org/10.2475/ajs.303.1.1
6. DeCelles, P.G.; Mitra, G. History of the Sevier orogenic wedge in terms of critical taper models, northeast Utah and southwest Wyoming. *Geol. Soc. Am. Bull.* **1995**, *107*, 454–462. https://doi.org/10.1130/0016-7606(1995)107<0454:HOTSOW>2.3.CO;2
7. Chapple, W.M. Mechanics of thin-skinned fold-and-thrust belt. *Geol. Soc. Am. Bull.* **1978**, *89*, 1189–1198. https://doi.org/10.1130/0016-7606(1978)89<1189:MOTFB>2.0.CO;2
8. Davis, D.; Suppe, J.; Dahlen, F.A. Mechanics of fold-and-thrust belts and accretionary wedges. *J. Geophys. Res.* **1983**, *88*, 1153–1172. https://doi.org/10.1029/JB088iB02p01153
9. Williams, C.A.; Conners, C.; Dahlen, F.A.; et al. Effect of the brittle – ductile transition on the topography of compressional mountain belts on Earth and Venus. *J. Geophys. Res.* **1994**, *99*, 19947–19974. https://doi.org/10.1029/94JB01407
10. Woodward, N.B. Geological applicability of critical-wedge thrust-belt models. *Geol. Soc. Am. Bull.* **1987**, *99*, 827–832. https://doi.org/10.1130/0016-7606(1987)99<827:GAOCTM>2.0.CO;2
11. Mitra, G. Evolution of salients in a fold-and-thrust belt: The effects

of sedimentary basin geometry, strain distribution and critical taper. In *Evolution of Geological Structures from Macro- to Micro-scales*; Sengupta, S., Ed.; Chapman and Hall: London, UK, 1997; pp. 59–90.

12. DeCelles, P.G. Late Cretaceous–Paleocene synorogenic sedimentation and kinematic history of the Sevier thrust belt, northeast Utah and southwest Wyoming. *Geol. Soc. Am. Bull.* **1994**, *106*, 32–56. https://doi.org/10.1130/0016-7606(1994)106<0032:LCPSSA>2.3.CO;2
13. Lawton, T.F. Lithofacies correlations within the Upper Cretaceous Indianola Group. In *Overthrust Belt of Utah*; Nielson, D. L., Ed.; Utah Geological Association Publication 10; Utah Geological Association: Salt Lake City, UT, USA, 1982; pp. 199–213.
14. Lawton, T.F. Style and timing of the frontal structures, Sevier thrust belt, central Utah. *AAPG Bull.* **1985**, *69*, 1145–1159. https://doi.org/10.1306/AD462B6F-16F7-11D7-8645000102C1865D
15. Mitra, G.; Sussman, A.J. Structural evolution of connecting splay duplexes and their implications for critical taper: An example based on geometry and kinematics of the Canyon Range culmination, Sevier Belt, central Utah. *J. Struct. Geol.* **1997**, *19*, 503–521. https://doi.org/10.1016/S0191-8141(96)00093-4
16. Naeser, C.W.; Bryant, B.; Crittenden, M.D. Jr.; et al. Fission-track ages of apatite in the Wasatch mountains. In *Tectonic and Stratigraphic Studies in the Eastern Great Basin*; Miller, D.M., Todd, V.R., Howard, K.R., Eds.; Geological Society of America Memoir 157; Geological Society of America: Boulder, CO, USA, 1983; pp. 29–36.
17. Boyer, S.E. Geometric evidence for synchronous thrusting in the southern Alberta and northwest Montana thrust belts. In *Thrust Tectonics*; McClay, K.R., Ed.; Chapman and Hall: London, UK, 1992; pp. 377–390.
18. Crider, J.G. Kinematic and Geometric Analysis of Meso-scale and Macro-scale Brittle Structures: Evolution of the Northern Sawtooth Range, Montana. M.S. Thesis, University of Washington, Seattle, USA, 1993.
19. Crider, J.G.; Boyer, S.E. Evidence for synchronous thrusting in the northern Sawtooth Range, Montana. *Abstr. Programs - Geol. Soc. Am.* **1993**, *25*, 25.
20. Boyer, S.E.; Mitra, G. Deformation of the basement-cover transition zone of the Appalachian Blue Ridge Province. In *Geometry and Mechanisms of Thrusting*; Mitra, G., Wojtal, S., Eds.; Geological Society of America Special Paper 222; Geological Society of America: Boulder, CO, USA, 1988; pp. 119–136.
21. Rodgers, J. *The Tectonics of the Appalachians*; Wiley-Interscience: New York, NY, USA, 1970; p. 271.
22. Gwinn, V.E. Kinematic patterns and estimates of lateral shortening, Valley and Ridge and Great Valley Provinces, Central Appalachians, South-Central Pennsylvania. In *Studies of Appalachian Geology, Central and Southern*; Fisher, G.W., Pettijohn, F.J., Reed, J.C., Jr., et al., Eds.; Geological Society of America: Boulder, CO, USA, 1970; pp. 127–146.
23. Mulugeta, G.; Koyi, H. Three-dimensional geometry and kinematics of experimental piggyback thrusting. *Geology* **1987**, *15*, 1052–1056. https://doi.org/10.1130/0091-7613(1987)15<1052:TGAKOE>2.0.CO;2
24. Colletta, B.; Letouzey, J.; Pinedo, R.; et al. Computerized x-ray tomography analysis of sandbox models: Examples of thin-skinned thrust systems. *Geology* **1991**, *19*, 1063–1067. https://doi.org/10.1130/0091-7613(1991)019<1063:CXRTAO>2.3.CO;2
25. Marshak, S.; Wilkerson, M.S. Effect of overburden thickness on thrust belt geometry and development. *Tectonics* **1992**, *11*, 560–566. https://doi.org/10.1029/92TC00175
26. Kwon, S.; Mitra, G.; Perucchio, R. Effect of predeformational basin geometry in the kinematic evolution of a thin-skinned orogenic wedge: Insights from three-dimensional finite element modeling of the Provo salient, Sevier fold-thrust belt, Utah. *J. Geophys. Res. Solid Earth* **2007**, *112*, B02403. https://doi.org/10.1029/2006JB004376
27. Mulugeta, G. Modelling the geometry of Coulomb thrust wedges. *J. Struct. Geol.* **1988**, *10*, 847–859. https://doi.org/10.1016/0191-8141(88)90099-5
28. Huiqi, L.; McClay, K.R.; Powell, D. Physical models of thrust wedges. In *Thrust Tectonics*; McClay, K.R., Ed.; Chapman & Hall: London, UK, 1992; pp. 71–81.
29. Graveleau, F.; Malavieille, J; Dominguez, F. Experimental modelling of orogenic wedges: A review. *Tectonophysics* **2012**, *538–540*, 1–66. https://doi.org/10.1016/j.tecto.2012.01.027
30. Boyer, S.E. Sedimentary basin taper as a factor controlling the geometry and advance of thrust belts. *Am. J. Sci.* **1995**, *295*, 1220–1254. https://doi.org/10.2475/ajs.295.10.1220
31. Sibson, R.H. Fault rocks and fault mechanisms. *J. Geol. Soc. Lond.* **1977**, *133*, 191–213. https://doi.org/10.1144/gsjgs.133.3.0191
32. Elliott, D. The motion of thrust sheets. *J. Geophys. Res.* **1976**, *81*, 949–963. https://doi.org/10.1029/JB081i005p00949
33. Remitti, F.; Festa, A.; Nirta, G.; et al. Role of folding-related deformation in the seismicity of shallow accretionary prisms. *Nat. Geosci.* **2024**, *17*, 600–607. https://doi.org/10.1038/s41561-024-01474-6
34. Nickelsen, R.P. Sequence of structural stages of the Alleghany orogeny at the Bear Valley Stripe Mine, Shamokin, Pennsylvania. *Am. J. Sci.* **1979**, *279*, 225–271. https://doi.org/10.2475/ajs.279.3.225
35. Geiser, P.A. Mechanisms of thrust propagation: Examples and implications for the analysis of overthrust terranes. *J. Struct. Geol.* **1988**, *10*, 829–845. https://doi.org/10.1016/0191-8141(88)90098-3
36. Oxburgh, E.R.; Turcotte, D.L. Thermal gradients and regional metamorphism in overthrust terranes with special reference to the Eastern Alps. *Schweiz. Mineral. Petrogr. Mitt.* **1974**, *54*, 641–662.
37. Lawton, T.F.; Boyer, S.E.; Schmitt, J.G. Influence of inherited taper on structural variability and conglomerate distribution, Cordilleran fold and thrust belt, western United States. *Geology* **1994**, *22*, 339–342. https://doi.org/10.1130/0091-7613(1994)022<0339:IOITOS>2.3.CO;2
38. Douglas, R.J.W. *Preliminary Map, Waterton, Alberta*; Canada Geological Survey Paper; Geological Survey of Canada: Ottawa, ON, Canada, 1952; pp. 51–22.
39. Spratt, D.A.; Simony, P.S.; Price, R.A.; et al. Fault-related folding in the Foothills and Front Ranges of Southern Alberta. In *Geological Society of America Penrose Conference Field Trip Guidebook*; Geological Society of America: Boulder, CO, USA, 1995; p. 95.
40. Heimgartner, D. Structural Geology of the Southern Termination of the Lewis Thrust Fault, Northwestern Montana. M.S. Thesis, University of Rochester, Rochester, NY, USA, 1997.
41. Constenius, K.N. Late Paleogene extensional collapse of the Cordilleran foreland fold and thrust belt. *Geol. Soc. Am. Bull.* **1996**, *108*, 20–39. https://doi.org/10.1130/0016-7606(1996)108<0020:LPECOT>2.3.CO;2
42. Price, R.A.; Sears, J.W. A preliminary palinspastic map of the Mesoproterozoic Belt-Purcell Supergroup, Canada and USA: Implications for the tectonic setting and structural evolution of the Purcell anticlinorium and the Sullivan deposit. In *The Geological Environment of the Sullivan Deposit, British Columbia*; Lydon, J.W., Höy, T., Slack, J.F., et al., Eds.; Geological Association of Canada, Mineral Deposits Division, Special Publication 1; Geological Association of Canada: Ottawa, ON, Canada, 2000; pp. 61–81.
43. Sears, J. Emplacement and denudation history of the Lewis-Eldorado-Hoadley thrust slab in the northern Montana Cordillera, USA: Implications for steady-state orogenic processes. *Am. J. Sci.* **2001**, *301*, 359–373. https://doi.org/10.2475/AJS.301.4-5.359
44. Ross, C.P. *Geology of Glacier National Park and the Flathead Region, Northwestern Montana*; U.S. Geological Survey Professional Paper 296; United States Geological Survey: Washington, DC, USA, 1959; p. 125.

45. Willis, B. Stratigraphy and structure, Lewis and Livingston Ranges, Montana. *Geol. Soc. Am. Bull.* **1902**, *13*, 305–352.
46. Ruhle, G.C. *Guide to Glacier National Park*, Campbell-Methun, Inc: Minneapolis, MN, USA, 1949; p. 189.
47. Yin, A.; Kelty, T.K.; Davis, G.A. Duplex abandonment and development during the evolution of the Lewis thrust system, Glacier National Park, Montana. *Geology* **1989**, *17*, 806–810. https://doi.org/10.1130/0091-7613(1989)017<0806:DDAADE>2.3.CO;2
48. Yin, A.; Kelty, T.K. Structural evolution of the Lewis thrust system, southern Glacier National Park: Implications for the regional tectonic development. *Geol. Soc. Am. Bull.* **1991**, *103*, 1073–1089. https://doi.org/10.1130/0016-7606(1991)103<1073:SEOTLP>2.3.C O;2
49. Dahlstrom, C.D.A. Structural geology in the eastern margin of the Canadian Rocky Mountains. *Bull. Can. Pet. Geol.* **1970**, *18*, 332–406. https://doi.org/10.1306/5D25CA81-16C1-11D7-8645000102C1865D
50. Fermor, P.R.; Price, R.A. *Imbricate Structures in the Lewis Thrust Sheet Around Cate Creek and Haig Brook Windows, Southeast British Columbia*; Canada Geological Survey Paper 76-1B; Geological Survey of Canada: Ottawa, ON, Canada, 1976; pp. 7–10.
51. Fry, N. Random point distributions and strain measurement in rocks. *Tectonophysics* **1979**, *60*, 89–105. https://doi.org/10.1016/0040-1951(79)90135-5
52. Erslev, E.A.; Ge, H. Least-squares center-to-center and mean object ellipse fabric analysis. *J. Struct. Geol.* **1990**, *12*, 201–209. https://doi.org/10.1016/0191-8141(90)90100-D
53. McNaught, M.A. Modifying the normalized Fry method for aggregates of non-elliptical grains. *J. Struct. Geol.* **1994**, *18*, 573–583. https://doi.org/10.1016/0191-8141(94)90043-4
54. Mukul, M.; Mitra, G. Finite strain and strain variation analysis in the Sheeprock thrust sheet, an internal thrust sheet in the Provo salient of the Sevier fold-and-thrust belt, central Utah. *J. Struct. Geol.* **1998**, *20*, 385–406. https://doi.org/10.1016/S0191-8141(97)00087-4
55. DeCelles, P.G.; Coogan, J.C. Regional structure and kinematic history of the Sevier fold-and-thrust belt, central Utah. *Geol. Soc. Am. Bull.* **2006**, *118*, 841–864. https://doi.org/10.1130/B25759.1
56. Ismat, Z.; Mitra, G. Folding by cataclastic flow: Evolution of controlling factors during deformation. *J. Struct. Geol.* **2005**, *27*, 2181–2203. https://doi.org/10.1016/j.jsg.2005.08.005
57. Royse, F., Jr. Detachment fold train, Reed Wash area, west flank San Rafael swell: An example of limb lengthening, roll-through folding process on the eastern margin of the Sevier thrust belt. The rocky Mountain Association of Geologists. *Mt. Geol.* **1996**, *33*, 45–64.
58. Boyer, S.E.; Mitra, G. Fold duplexes. *J. Struct. Geol.* **2019**, *125*, 202–212. https://doi.org/10.1016/j.jsg.2018.07.008
59. Hintze, L.F. *Geologic History of Utah*; Brigham Young University Geology Studies Special Publication 7; Brigham Young University: Provo, UT, USA, 1988; p. 202.
60. Burchfiel, B.C.; Hickox, C.W. Structural development of central Utah. In *Plateau–Basin and Range Transition Zone, Central Utah*; Baer, J.L., Callaghan, E., Eds.; Geological Association Publication 2; Utah Geological Association: Salt Lake City, UT, USA, 1972; pp. 55–66.
61. Villien, A.; Kligfield, R.M. Thrusting and synorogenic sedimentation in central Utah. In *Paleotectonics and Sedimentation in the Rocky Mountain Region, United States*; Peterson, J.A., Ed.; Memoir 41; American Association of Petroleum Geologists: Tulsa, OK, USA, 1986; pp. 281–308.
62. Allmendinger, R.W.; Sharp, J.W.; Von Tish, D.; et al. Cenozoic and Mesozoic structure of the eastern Basin and Range province, Utah, from COCORP seismic reflection data. *Geology* **1983**, *11*, 532–536. https://doi.org/10.1130/0091-7613(1983)11<532:CAMSOT>2.0.CO;2
63. Coogan, J.C.; DeCelles, P.G. Extensional collapse along the Sevier Desert reflection, northern Sevier Desert basin, western United States. *Geology* **1996**, *24*, 933–936. https://doi.org/10.1130/0091-7613(1996)024<0933:ECATSD>2.3.CO;2
64. Standlee, L.A. Structure and stratigraphy of Jurassic rocks in central Utah: Their influence on tectonic development of the Cordilleran foreland thrust belt. In *Geologic Studies of the Cordilleran Foreland Thrust Belt*; Powers, R.B., Ed.; Rocky Mountain Association of Geologists: Denver, CO, USA, 1982; pp. 357–382.
65. Kwon, S.; Mitra, G. Strain distribution, strain history and kinematic evolution associated with the formation of arcuate salients in fold-thrust belts: The example of the Provo salient, Sevier orogen, Utah. In *Orogenic Curvature*; Sussman, A., Weil, A., Eds.; Geological Society of America Special Paper 383; Geological Society of America: Boulder, CO, USA, 2004; pp. 205–223.
66. Christie-Blick, N.H. Structural geology of the southern Sheeprock Mountains, Utah: Regional significance. In *Tectonics and Stratigraphic Studies in the Eastern Great Basin*; Miller, D.M., Todd, R., Howard, K.A., Eds.; Geological Society of America Memoir 157; Geological Society of America: Boulder, CO, USA, 1983; pp. 101–124.
67. Mukul, M.; Mitra, G. *Geology of the Sheeprock Thrust Sheet, Central Utah -New Insights*; Utah Geological Survey Miscellaneous Publications 98-1; Utah Geological Survey: Salt Lake City, UT, USA, 1998; p. 56.
68. Kwon, S.; Mitra, G. Three-dimensional finite-element modeling of a thin-skinned fold-thrust belt wedge: Provo salient, Sevier belt, Utah. *Geology* **2004**, *32*, 561–564. https://doi.org/10.1130/G20415.1
69. Strine, M.; Mitra, G. Preliminary kinematic data from a salient-recess pair along the Moine thrust, northwest Scotland. In *Orogenic Curvature*; Sussman, A., Weil, A., Eds.; Geological Society of America Special Paper 383-14; Geological Society of America: Boulder, CO, USA, 2004; pp. 87–107.
70. Kwon, S.; Mitra, G. Three-dimensional kinematic history at an oblique ramp: The Leamington Zone of the Sevier FTB as an example. *J. Struct. Geol.* **2006**, *28*, 474–493. https://doi.org/10.1016/j.jsg.2005.12.011
71. Paulsen, T.; Marshak, S. Origin of the Uinta recess, Sevier fold-thrust belt, Utah: Influence of basin architecture on fold-thrust belt geometry. *Tectonophysics* **1999**, *312*, 203–216. https://doi.org/10.1016/S0040-1951(99)00182-1